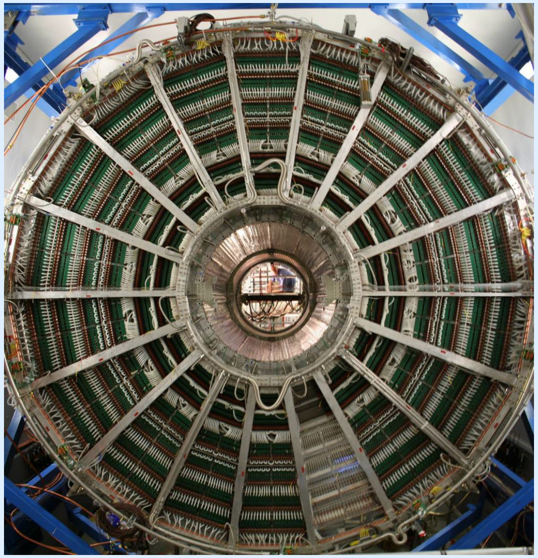

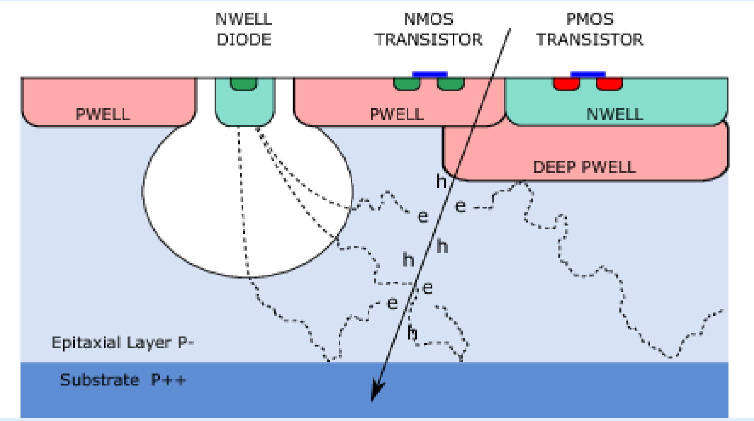

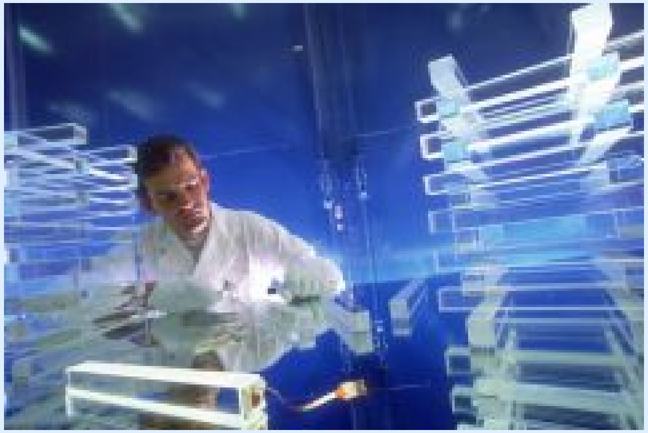

Electromagnetic and hadronic calorimeters

Silvia Masciocchi
GSI Darmstadt and University of Heidelberg

39th Heidelberg Physics Graduate Days, HGSFP
Heidelberg
October 12, 2017

Calorimetry

Experimental technique in nuclear and particle physics in which the detection of a particle and the measurement of its properties is based on ABSORPTION in the detector volume (partial or total)

This is a **DESTRUCTIVE** process:

The particle's energy is converted in a detectable signal until the particle is absorbed

Another note: calorimetry is addressed also to **neutral particles** (not only charged one, see magnetic spectrometer)

Electromagnetic calorimeters: outline

- Introduction
  - Energy measurement: total absorption of the particle energy via shower production ...
  - … particularly targeted to high momentum/energy particles
- Electromagnetic shower
  - Electron bremsstrahlung and photon pair production
  - Transverse and longitudinal shower development
- Electromagnetic calorimeters
  - Homogeneous and sampling calorimeters
  - Energy resolution

Introduction

Measurement of energy or momentum of particles:

Let's focus on high energy particles (hadrons, leptons, (photons))

Magnetic spectrometers

Momentum of charged particles is measured in magnetic field, with tracking detectors to determine the trajectory

$$\frac{\sigma_p}{p} \propto \frac{p}{L^2}$$

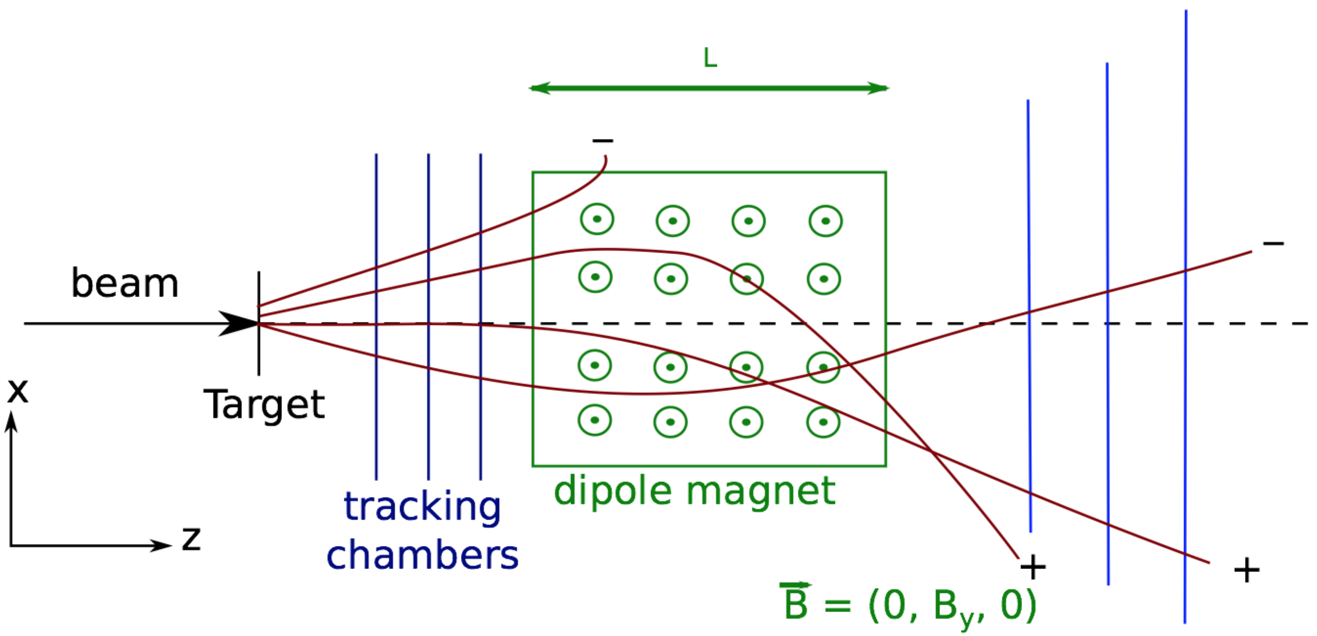

This is NOT the best choice to measure high energy particles.

With increasing p (or E), the momentum resolution gets worse, or an impossibly long lever arm L is needed → switch to **calorimeters** !

Introduction

Calorimeters are the ideal instrument to measure the full energy of particles, particularly at high momentum

$$\frac{\sigma_E}{E} \propto \frac{1}{\sqrt{E}}$$

Resolution improves with energy!

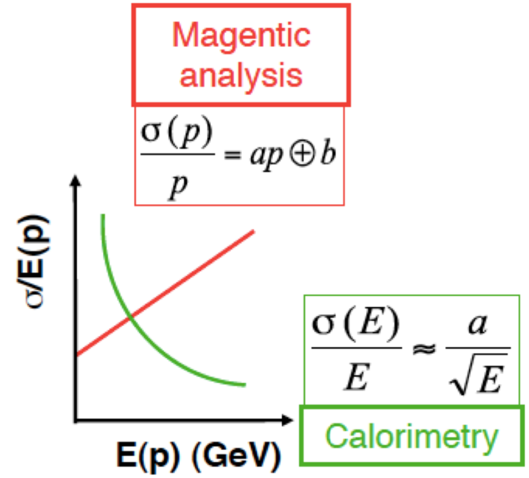

Other advantages:

- Depth of shower $\propto$ ln (E/E_0) → grows only with ln(E) (while the momentum resolution would be “controlled” only by L^2 → unfeasible in reality)
- Calorimeter can cover full solid angle
- Fast timing signal from calorimeter → can be used for triggering!
- Distinction of hadronic and electromagnetic showers using segmentation in depth

What do calorimeters measure?

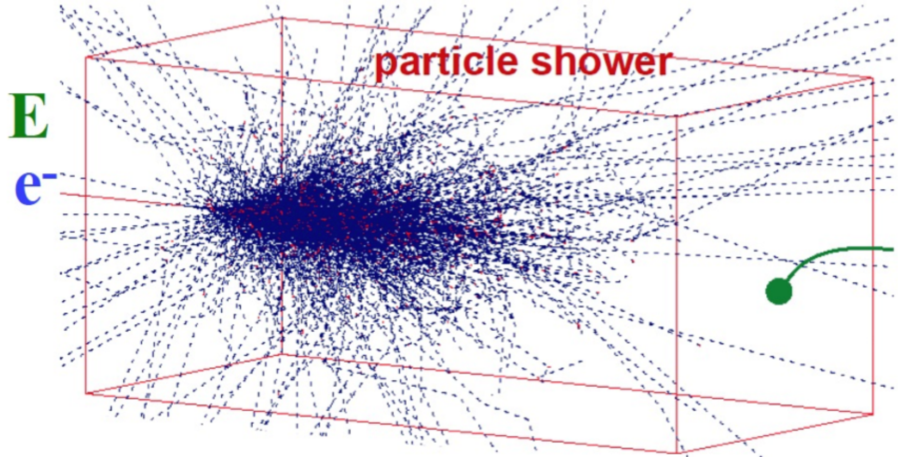

- An incident particle interacts with the calorimeter active and passive material
- A cascade process is initiated: shower development depends on particle type and on detector material
- Visible energy deposited in the active media of the calorimeter produces a detectable signal, proportional to the total energy deposited by the particle
- Essential to CALIBRATE the calorimeter, namely establish a precise relationship between the “visible energy” detected and the energy of the incoming particle

Introduction: classification of calorimeters

By particle type:

- Electromagnetic calorimeters: electrons, positrons, photons, π^0
- Hadronic calorimeters: charged and neutral hadrons, jets

By construction techniques:

- Homogeneous calorimeters: full absorption detectors, fully active medium for both energy degradation and signal generation
- Sampling calorimeters: alternate layers of absorber material to degrade the particle energy and active media to provide the detectable signal

Electromagnetic shower

Electrons (positrons) and photons interacting with matter

Big European Bubble Chamber filled with Ne:H_2 = 70%:30%, 3T Field, L=3.5 m, $X_0 \approx 34$ cm, 50 GeV incident electron

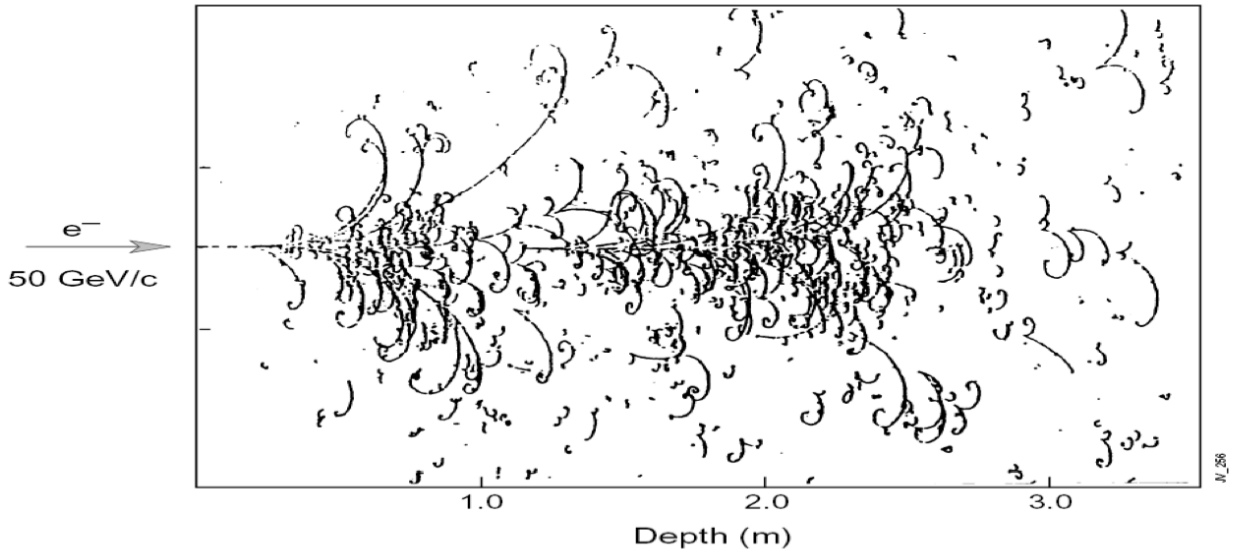

PbW0$_4$ CMS, X_0=0.89 cm

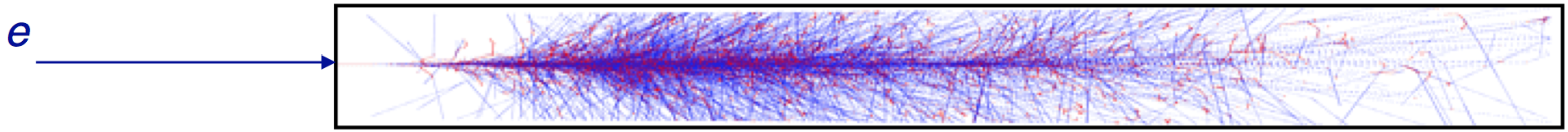

Electromagnetic shower: electrons

Electrons have two dominant effects through which they loose energy in their interaction with matter:

- ionization / excitation of atoms → Bethe-Bloch

  after the minimum around βγ ≈ 3, the rise is weak and the dE/dx remains relatively low

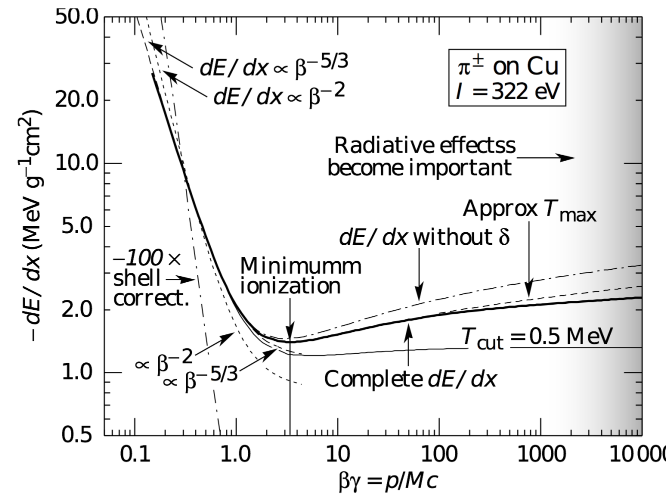

- Bremsstrahlung:

  X_0 = radiation length

$$\frac{dE}{dx} = -\frac{E}{X_0}$$

$$E = E_0 \exp(-x/X_0)$$

Moliere radius (relevant for transverse size of the shower)

$$R_M = \frac{21.2\,\text{MeV}}{E_c} \cdot X_0$$

→ Critical energy E_c !!

Critical energy

Total energy loss of electrons:

$$\left(\frac{dE}{dx}\right)_{Tot} = \left(\frac{dE}{dx}\right)_{Ion} + \left(\frac{dE}{dx}\right)_{Brems}$$

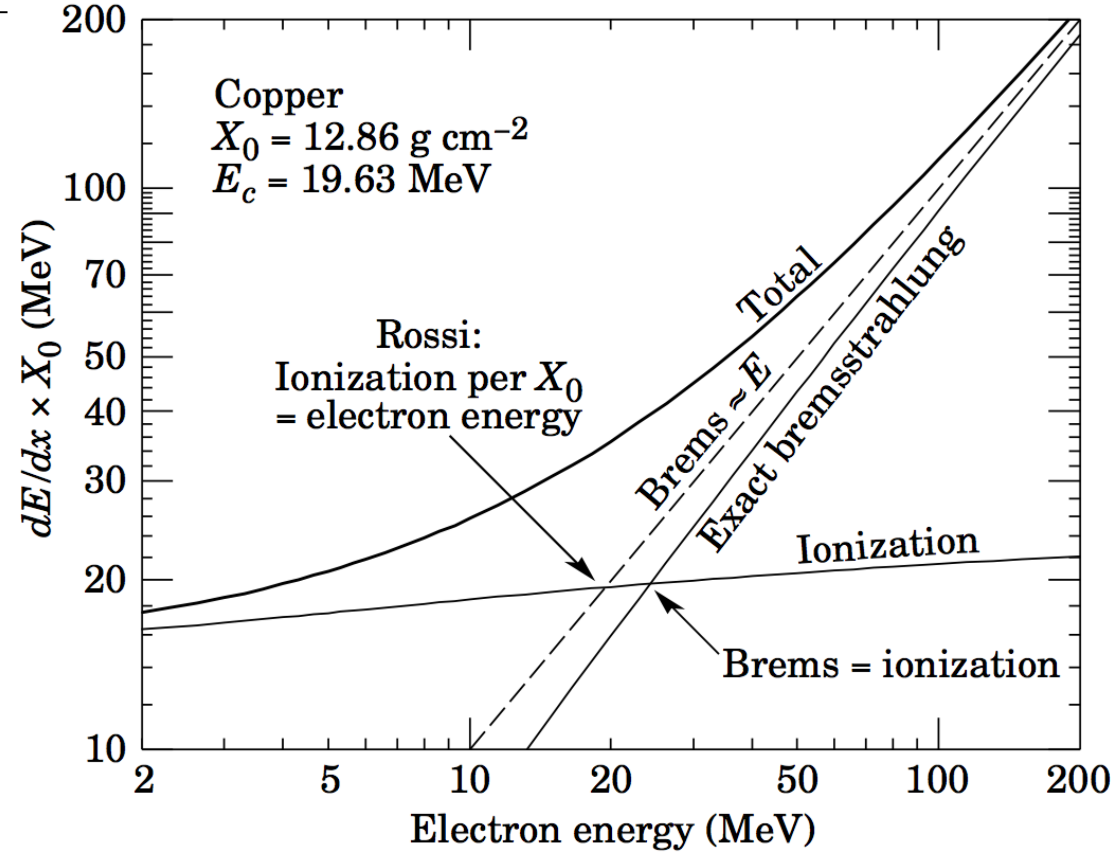

Critical energy:

$$\left(\frac{dE}{dx}(E_c)\right)_{Brems} = \left(\frac{dE}{dx}(E_c)\right)_{Ion}$$

Example: Cu $E_c \approx 610/30$ MeV ≈ 20 MeV

For E > E_c Bremsstrahlung dominates !!!

Photons

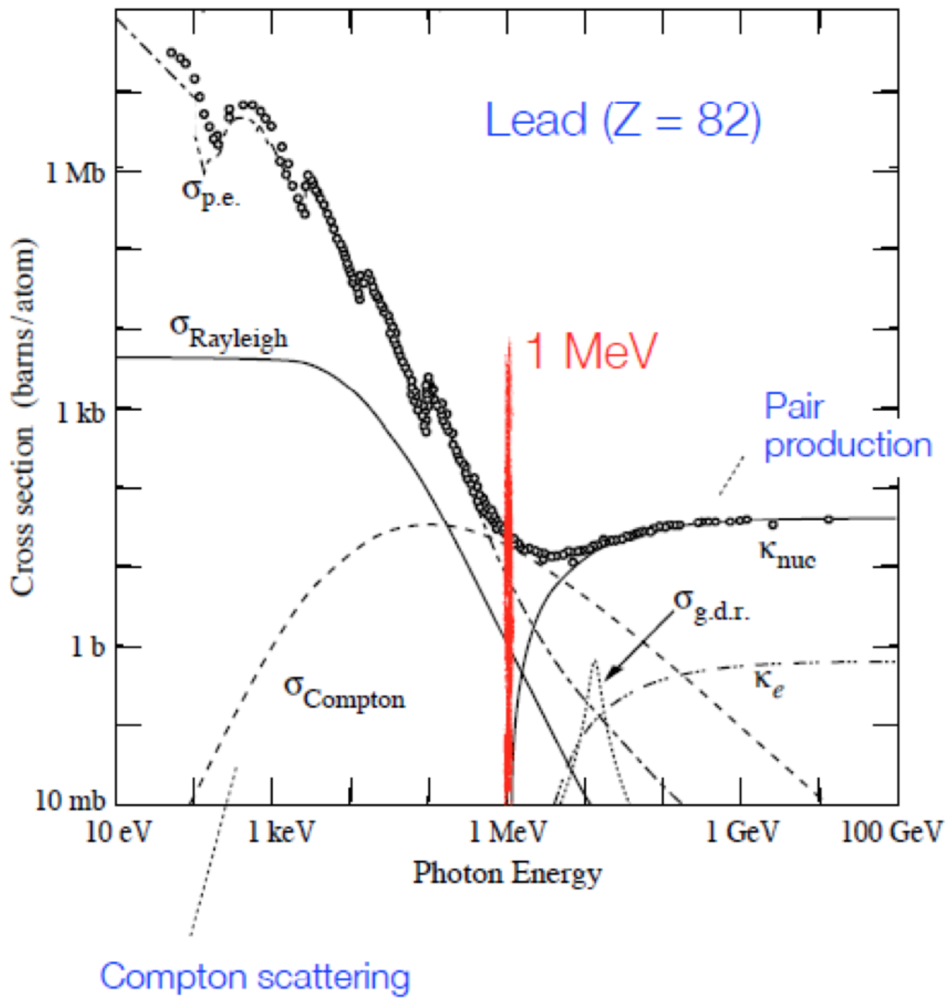

Dominant effect for energies above a few MeV:

Pair production

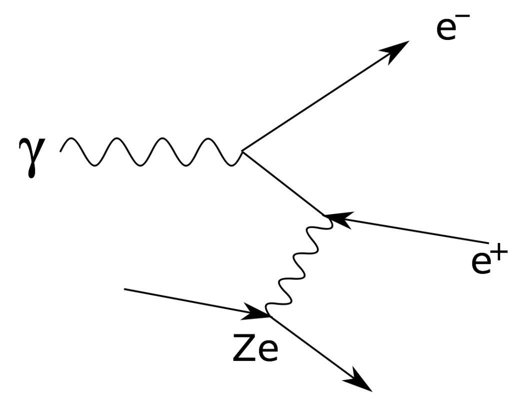

Probability for pair production (PP):

$$\frac{d\omega}{dx} = \frac{1}{\lambda_{PP}} e^{-x/\lambda_{PP}} \quad \rightarrow \quad \lambda_{PP} = \frac{9}{7} X_0$$

Electromagnetic shower

X_0 is the characteristic scale

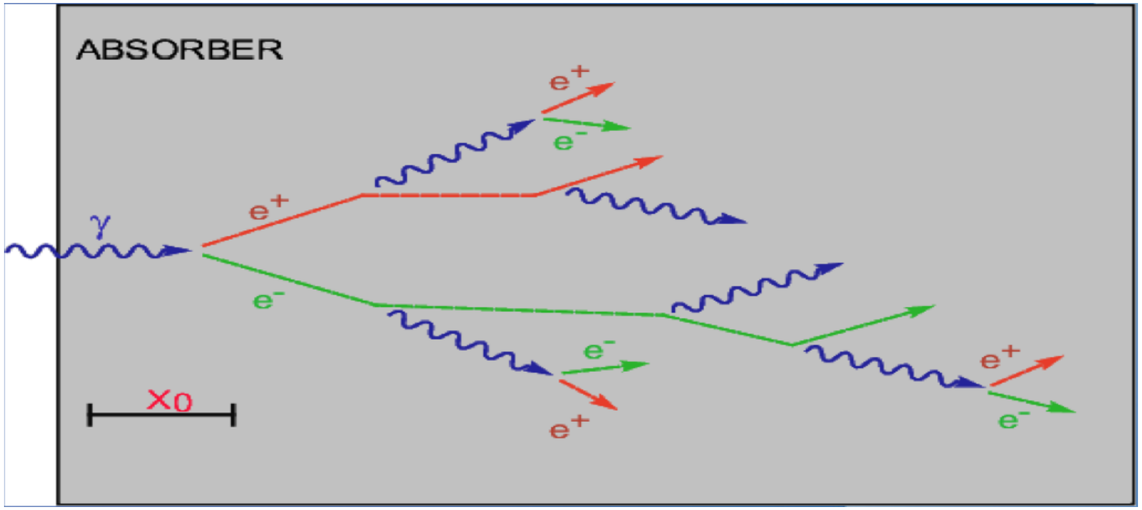

L.Fussel 1939

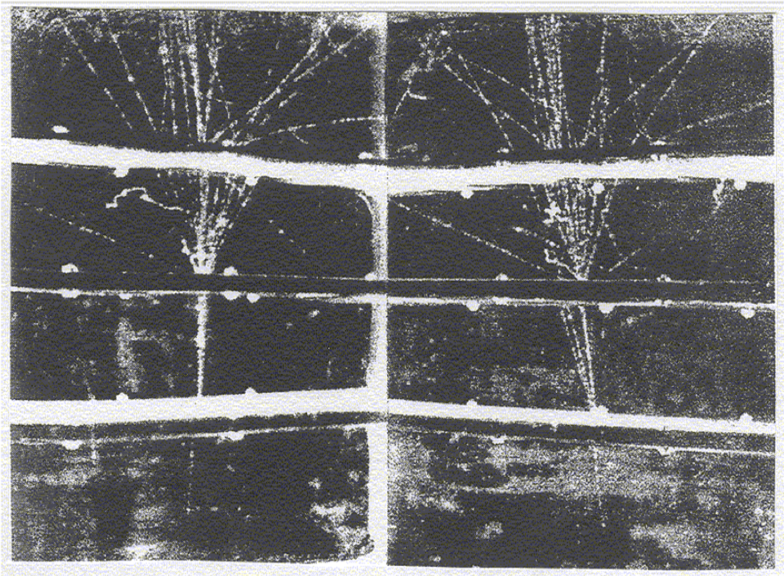

Electron Shower

L.Fussel 1939

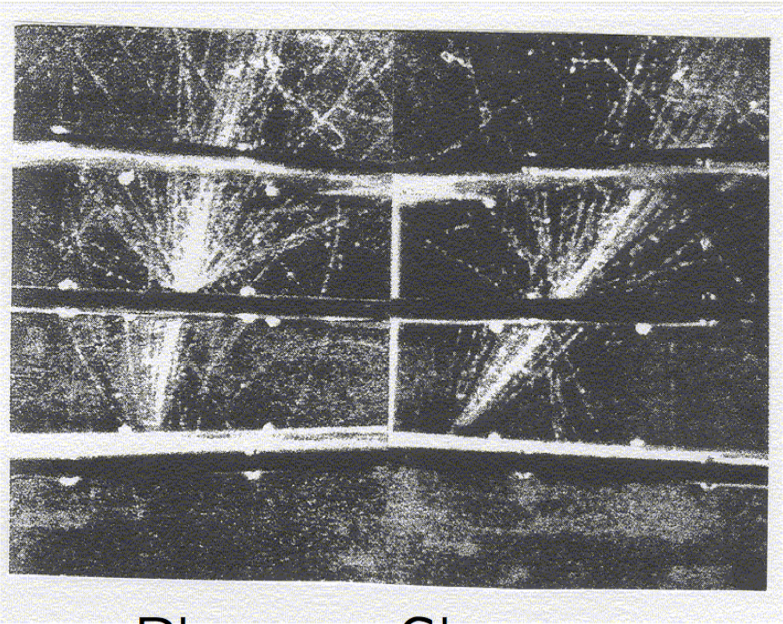

Photon Shower

Examples of used materials

material	Z	X_0 [g cm^{-2}]	X_0 [cm]	E_c [MeV]	R_M [cm]
plastic scint.			34.7	80	9.1
Ar (liquid)	18	19.55	13.9	35	9.5
Fe	26	13.84	1.76	21	1.77
BGO		7.98	1.12	10	2.33
Pb	82	6.37	0.56	7.4	1.60
U	92	6.00	0.32	6.8	1.00
Pb glass (SF5)			2.4	11.8	4.3

Analytic model of electromagnetic shower

A high energy electron/photon (above ~100 MeV) enters matter:

- Electron looses energy by Bremsstrahlung
  e + nucleus $\rightarrow$ e + γ + nucleus
- Photon is absorbed by pair production
  γ + nucleus $\rightarrow$ $e^+ + e^-$ + nucleus

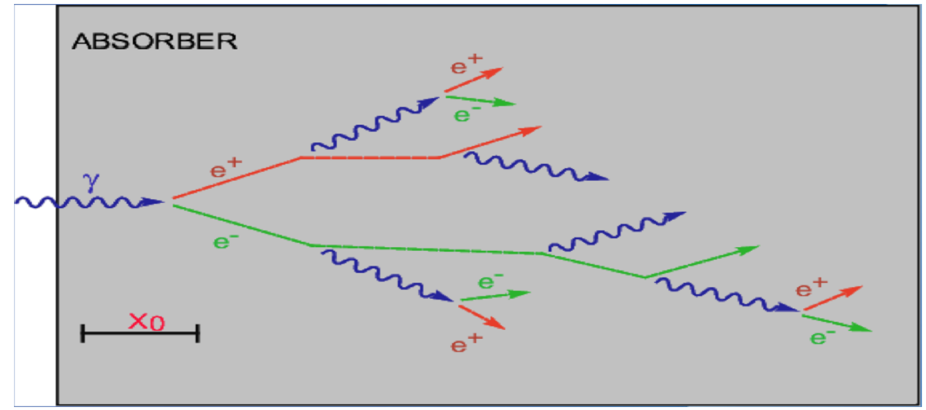

Approximate model:

- Over distance X_0, electron reduces via bremsstrahlung its energy to 1/e: $E_1 = E_2/e$
- Over distance ~X_0, photon converts to e^+e^-
  Energy of electron and positron: $E_\pm \simeq E_0/2$
  (precisely $\lambda_{PP} = 9/7X_0$. Pair production probability in X_0 is $P = 1 - \exp(-7/9)=0.54$)

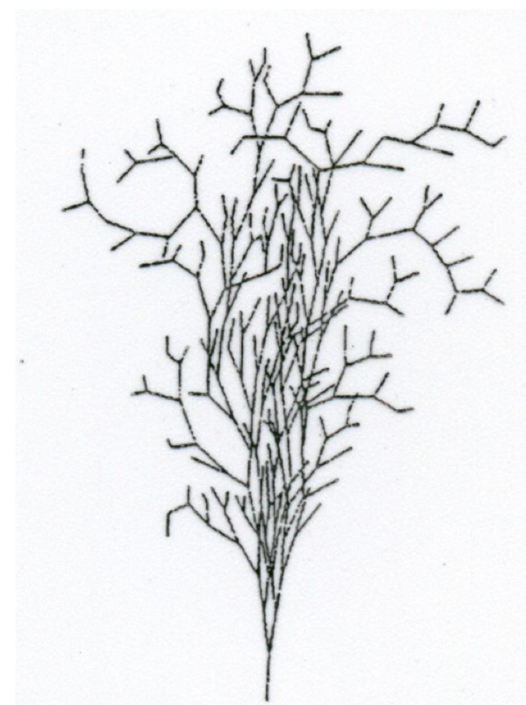

Assumptions:

- For $E>E_c$ no energy loss by ionization/excitation
- For $E<E_c$ electrons loose energy only via ionization/excitation

Analytic model of electromagnetic shower

An electromagnetic shower is characterized by:

- Number of particles in the shower
- Location of shower maximum
- Longitudinal shower distribution
- Transverse shower distribution

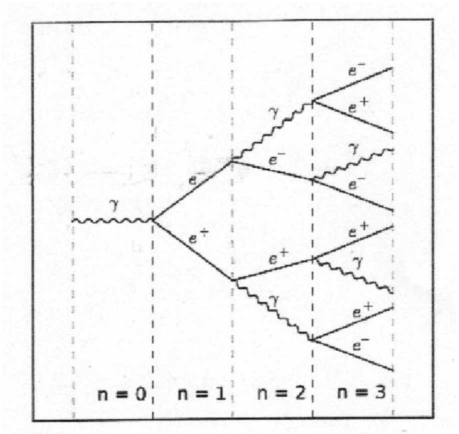

Simplified model (assuming e ≈ 2):

Introduce longitudinal variable $t = x/X_0$

Number of particles after traversing depth t:

$$N(t) = 2^t$$

Each particle has energy:

$$E(t) = \frac{E_0}{N(t)} = \frac{E_0}{2^t} \rightarrow t = \ln(E_0/E)/\ln 2$$

The shower ends approximately when $E \approx E_c$:

$$E_c = E(t_{max}) = \frac{E_0}{2^{t_{max}}}$$

$$2^{t_{max}} = E_0/E_c$$

Maximum shower depth:

$$t_{max} = \ln(E_0/E_c)/\ln 2$$

Maximum number of particles in shower:

$$N_{max} = \exp(t_{max}\ln 2) = E_0/E_c$$

Example: 1 GeV photon in CsI crystal: $E_c \simeq 10$ MeV, $N_{max} = E_0/E_c \simeq 100$, $t_{max} \simeq 6.6\ X_0$

Transverse shower development

- Emission of bremsstrahlung under SMALL angle $\langle \theta^2 \rangle \approx \frac{m}{E} = \frac{1}{\gamma^2}$
- 3D multiple scattering of electron in Moliere theory

$$\langle \theta_m^2 \rangle = \left(\frac{21.2\,\mathrm{MeV}}{\beta p c} \right)^2 t$$

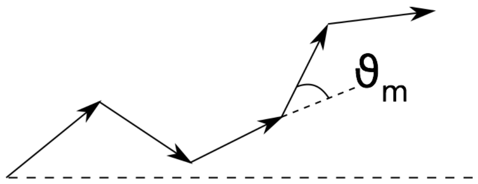

Multiple scattering dominates the transverse shower development!!

The main contribution comes from low energy electrons, assuming approximate range of electrons to be X_0

Moliere radius: $$R_M = \sqrt{\langle \theta^2 \rangle_{x=X_0} \cdot X_0} \approx \frac{21\,\mathrm{MeV}}{E_c} X_0$$

Transverse shower development

Useful relations:

$$X_0 = \frac{180A}{Z^2}(\mathrm{g\ cm^{-2}})$$

$$E_c = \frac{580\ \mathrm{MeV}}{Z}$$

$$t_{max} = \ln\frac{E}{E_c} - \begin{cases} 1 & e\ \text{induced shower} \\ 0.5 & \gamma\ \text{induced shower} \end{cases}$$

95% of energy within:

$L(95\%) = t_{max} + 0.08\,Z + 9.6\,X_0$

$R(95\%) = 2\,R_M$

a 6 GeV electron in lead

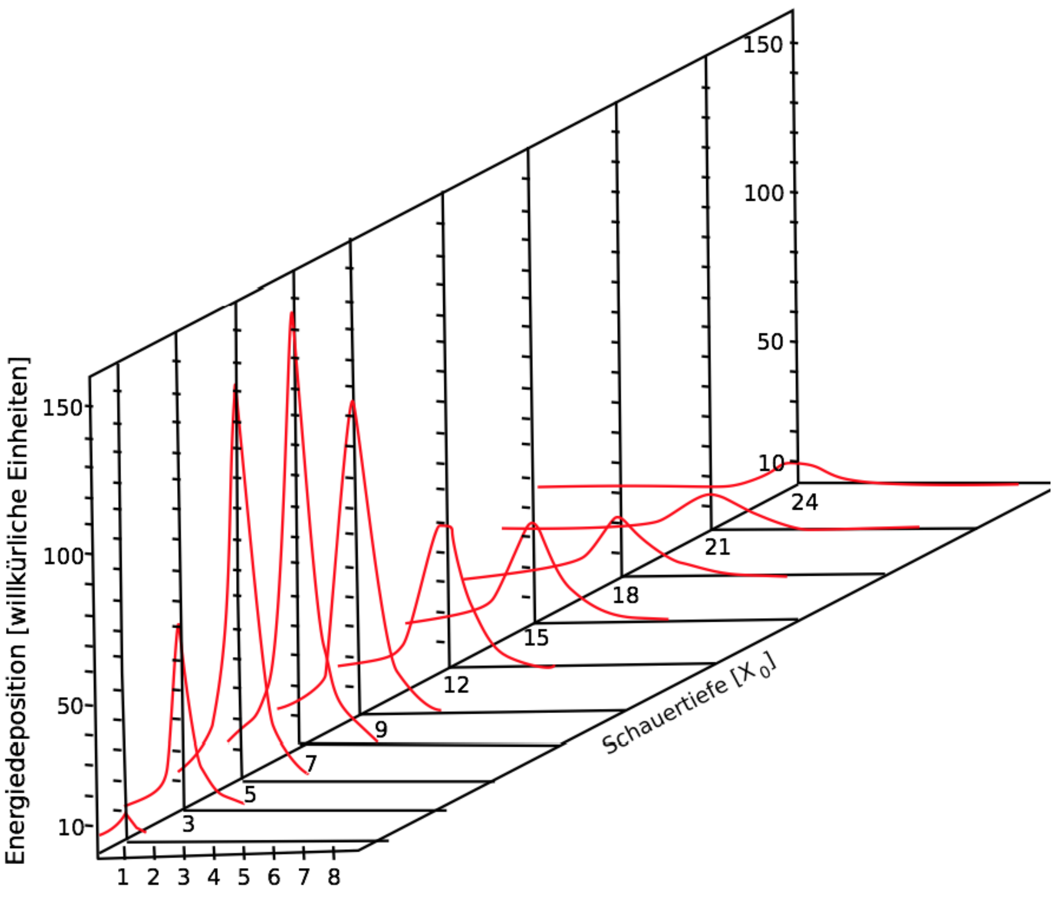

Longitudinal shower profile

Parametrization (Longo 1975)

$$\frac{dE}{dt} = E_0 t^{\alpha} \exp(-\beta t)$$

- First increase of secondaries
- Then absorption dominates

Energy deposit

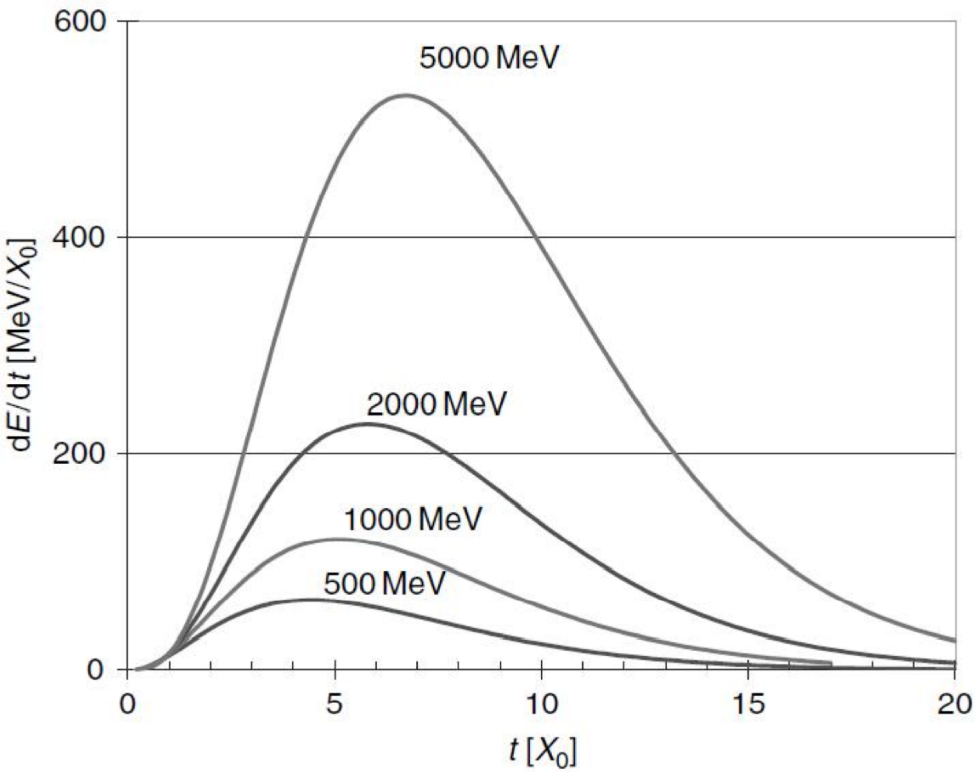

Remember:

- Most of the energy of the incident γ is absorbed in 10-15 X_0
- The max position increases slowly with E_0 (~ lnE, not E!)
- Energy leakage mostly due to soft photons at the sides and the back

Electromagnetic calorimeters

- Homogeneous calorimeters: full absorption detectors, fully active medium for both energy degradation and signal generation

- Sampling calorimeters: alternate layers of absorber material to degrade the particle energy and active media to provide the detectable signal

Electromagnetic calorimeters

Homogeneous Calorimeters
- Scintillation/ Crystal
- Semiconductor
- Cherenkov
- Ionization (Noble Liquids)

Sampling Calorimeters
- Scintillation
- Gas
- Solid State
- Liquids

Common Absorbers:

Pb, Fe, Cu, U

Existing Electromagnetic Calorimeters

Technology/Experiment	Depth	Resolution	Year
NaI(Tl) (Crystal Ball)	$20X_0$	$2.7\%/E^{1/4}$	1983
$Bi_4Ge_3O_{12}$ (BGO) (L3)	$22X_0$	$2\%/\sqrt{E} \oplus 0.7\%$	1993
CsI (KTeV)	$27X_0$	$2\%/\sqrt{E} \oplus 0.45\%$	1996
CsI(Tl) (BaBar)	16–$18X_0$	$2.3\%/E^{1/4} \oplus 1.4\%$	1999
CsI(Tl) (BELLE)	$16X_0$	1.7% for $E_\gamma > 3.5$ GeV	1998
$PbWO_4$ (PWO) (CMS)	$25X_0$	$3\%/\sqrt{E} \oplus 0.5\% \oplus 0.2/E$	1997
Lead glass (OPAL)	$20.5X_0$	$5\%/\sqrt{E}$	1990
Liquid Kr (NA48)	$27X_0$	$3.2\%/\sqrt{E} \oplus 0.42\% \oplus 0.09/E$	1998
Scintillator/depleted U (ZEUS)	20–$30X_0$	$18\%/\sqrt{E}$	1988
Scintillator/Pb (CDF)	$18X_0$	$13.5\%/\sqrt{E}$	1988
Scintillator fiber/Pb spaghetti (KLOE)	$15X_0$	$5.7\%/\sqrt{E} \oplus 0.6\%$	1995
Liquid Ar/Pb (NA31)	$27X_0$	$7.5\%/\sqrt{E} \oplus 0.5\% \oplus 0.1/E$	1988
Liquid Ar/Pb (SLD)	$21X_0$	$8\%/\sqrt{E}$	1993
Liquid Ar/Pb (H1)	20–$30X_0$	$12\%/\sqrt{E} \oplus 1\%$	1998
Liquid Ar/depl. U (DØ)	$20.5X_0$	$16\%/\sqrt{E} \oplus 0.3\% \oplus 0.3/E$	1993
Liquid Ar/Pb accordion (ATLAS)	$25X_0$	$10\%/\sqrt{E} \oplus 0.4\% \oplus 0.3/E$	1996

Homogeneous em calorimeters

Absorbing material ≡ detection material

- Scintillating crystals (sodium iodide NaI, bismuth germanate BGO, caesium iodide CsI, lead tungstate $PbWO_4$, etc.)

	NaI(Tl)	BGO	CsI(Tl)	$PbWO_4$
density (g/cm^3)	3.67	7.13	4.53	8.28
X_0 (cm)	2.59	1.12	1.85	0.89
R_M (cm)	4.5	2.4	3.8	2.2
dE/dx_{mip} (MeV/cm)	4.8	9.2	5.6	13.0
light yield (photons/MeV)	$4 \cdot 10^4$	$8 \cdot 10^3$	$5 \cdot 10^4$	$3 \cdot 10^2$
energy resolution σ_E/E	$1\%/\sqrt{E}$	$1\%/\sqrt{E}$	$1.3\%/\sqrt{E}$	$2.5\%/\sqrt{E}$

- Energy loss by ionization (noble liquids)
- Cherenkov (lead glass SF5)

Energy resolution of homogeneous calo

Contributions to the energy resolution σ_E/E:

- Shower fluctuations (intrinsic) stochastic term $\propto \frac{1}{\sqrt{E}}$
- photon/electron statistics in photon detector $\propto \frac{1}{\sqrt{E}}$
- Electronic noise $\propto \frac{1}{E}$
- Leakage, calibration $\simeq$ constant

Total energy resolution of electromagnetic calorimeter:

$$\boxed{\frac{\sigma_E}{E} = \frac{A}{\sqrt{E}} \oplus \frac{B}{E} \oplus X}$$

Examples

- PHOS in ALICE ($PbWO_4$ crystals)
- $PbWO_4$ calorimeter in CMS
- Alternative to scintillators → Cherenkov radiator e.g. lead glass

PHOS: PHOton Spectrometer in ALICE

Array of 22 x 22 x 180 cm^3 $PbWO_4$ crystals.
Depth = 20 X_0. Total ~ 18,000 crystals.

Characteristics: dense, fast, relatively radiation hard

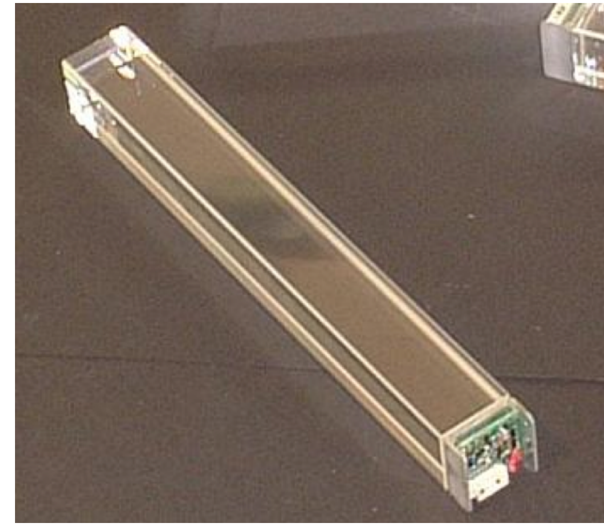

Emission spectrum: 420-550 nm

Readout: 5x5 mm^2 avalanche photodiodes, Q=85%

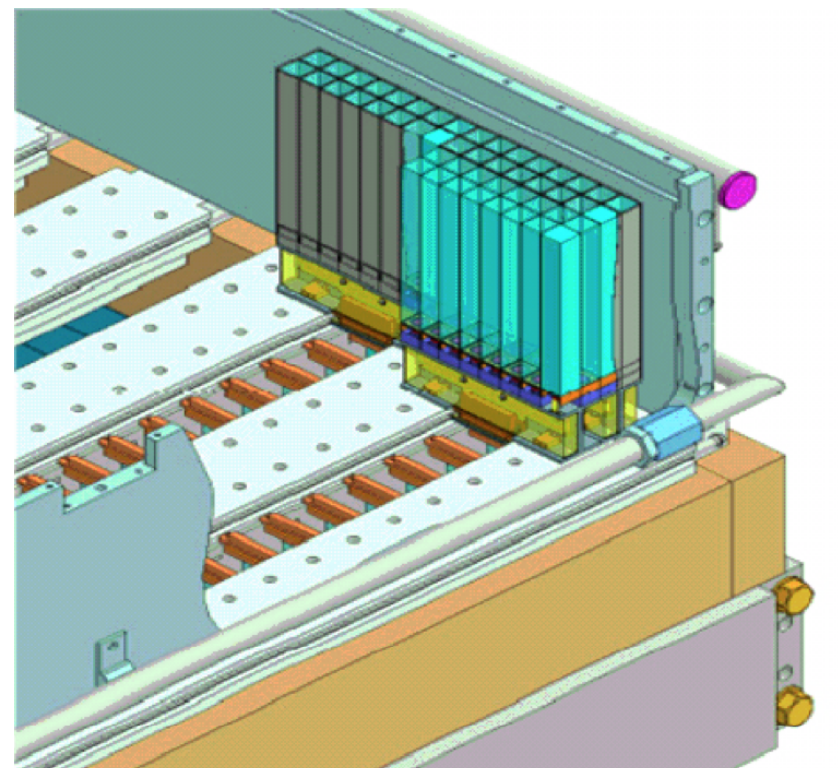

Light yield of $PbWO_4$ relatively low and strongly temperature dependent!!

Operate detector at -25º C, need to stabilize to 0.3º C (monitor with resistive temperature sensors)

Crystals cold, electronics warm

PHOS in ALICE

12.5 t of crystals, covering 8m^2 at 4 m from beam line

In front: charged particle veto – MWPC with cathode pad readout

Test beams of pions and electrons at CERN PS and SPS: 0.6 – 150 GeV

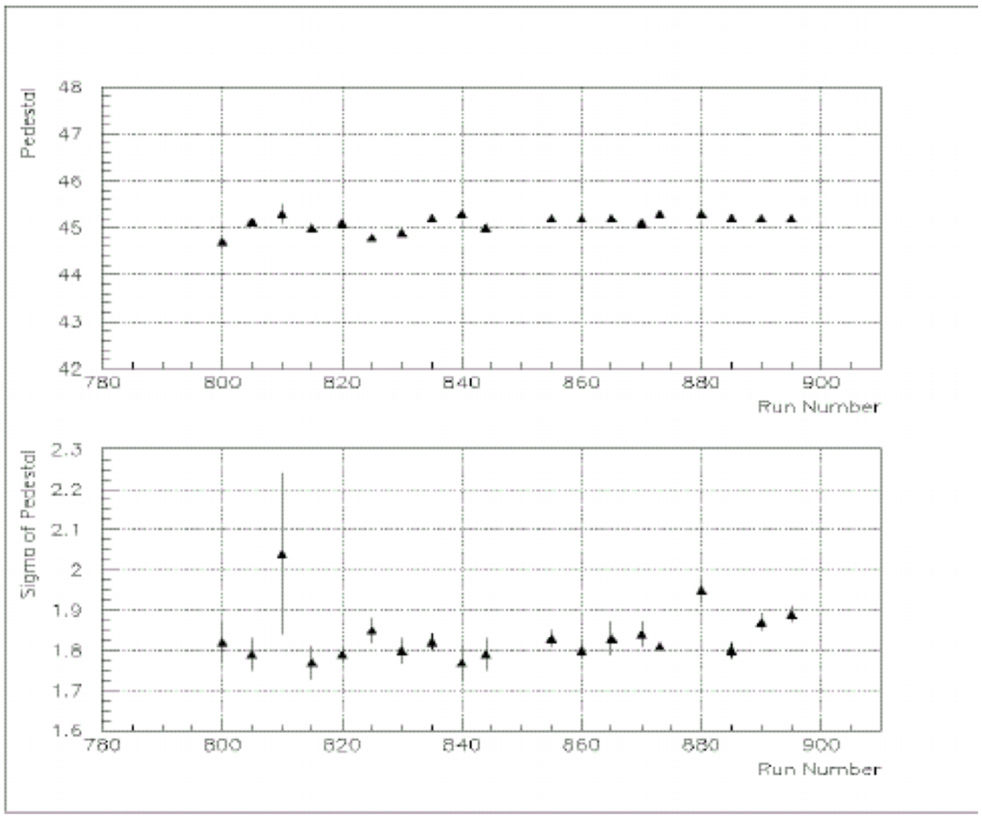

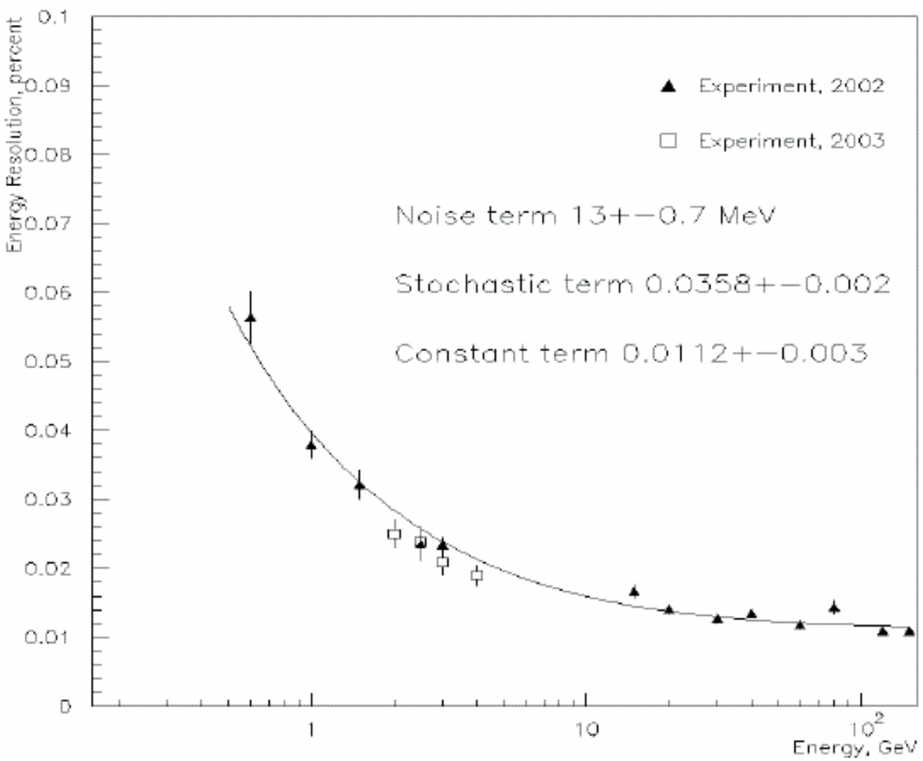

electronic noise:
1 ch = 400 e → noise about 700 e

$$\frac{\sigma_E}{E} = \frac{3.6\%}{\sqrt{E}} \oplus \frac{1.3\%}{E} \oplus 1.1\%$$

Importance of energy resolution

Peaks sit on combinatorial background. S/B depends on resolution

$\pi^0, \eta \rightarrow \gamma\gamma$

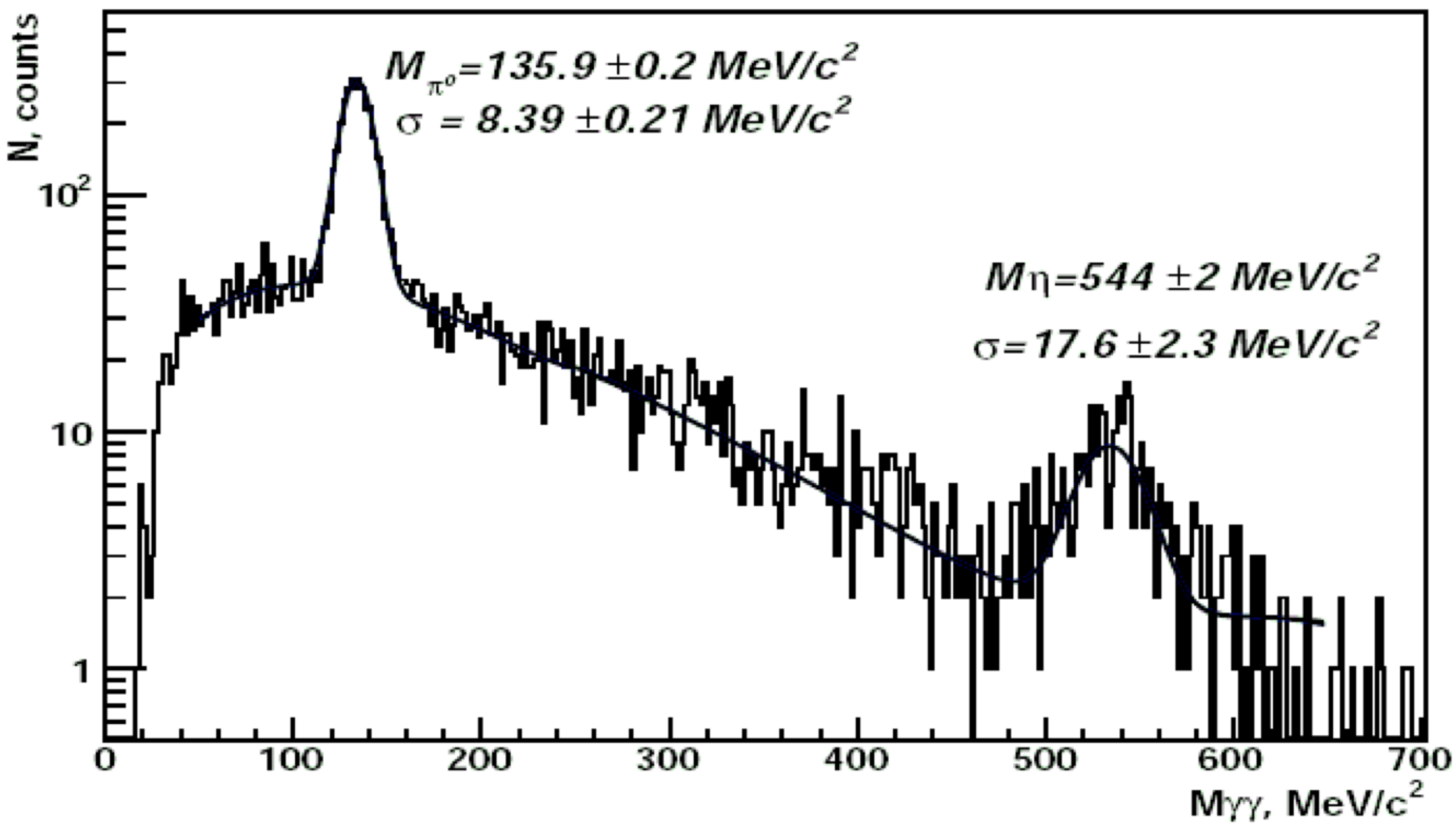

Invariant mass spectrum from the inclusive reaction:

6 GeV/c $\pi^- + {}^{12}C \rightarrow \pi^0 + X$

measured at 122 cm distance

CMS crystal calorimeter ($PbWO_4$)

Most important Higgs discovery channel:

$H \rightarrow \gamma\gamma$

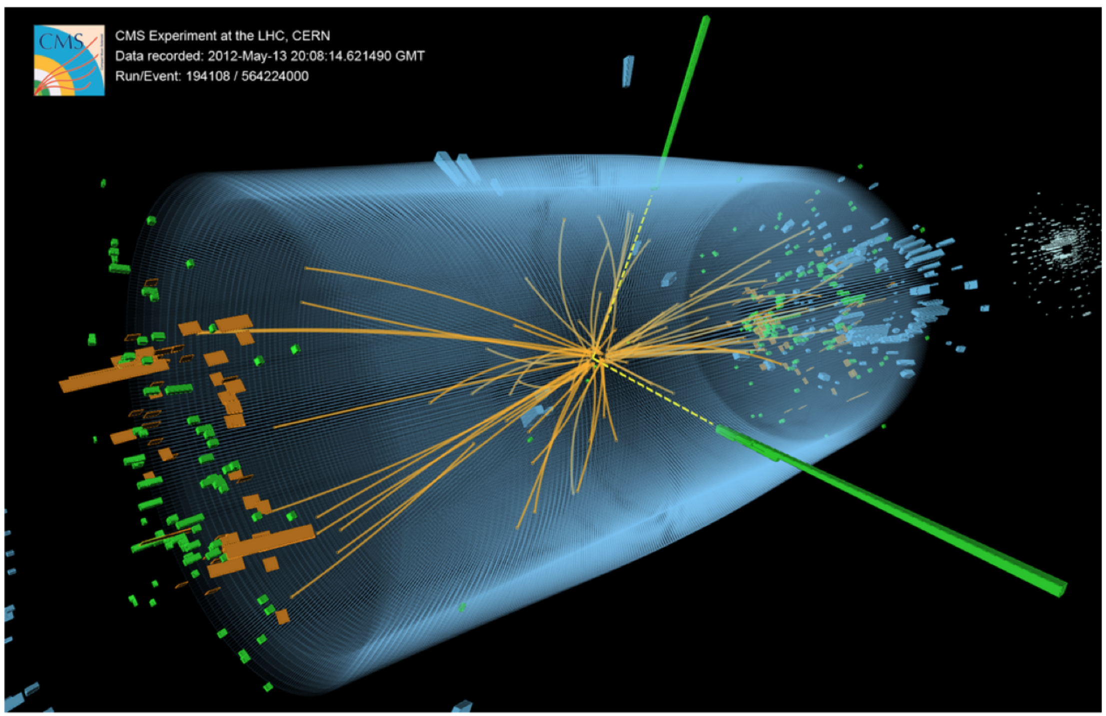

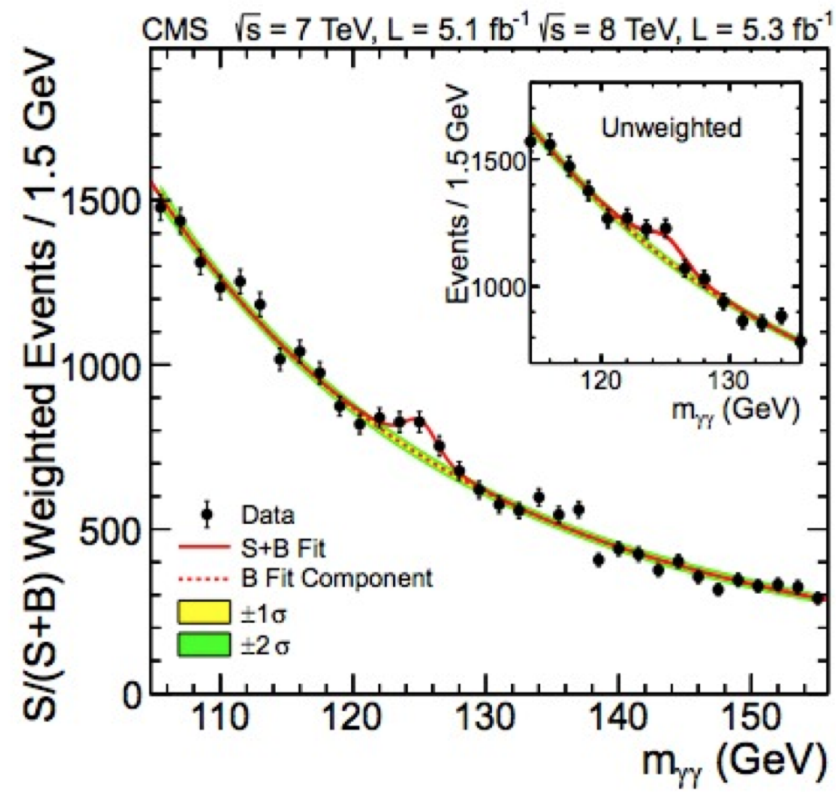

CMS crystal calorimeter ($PbWO_4$)

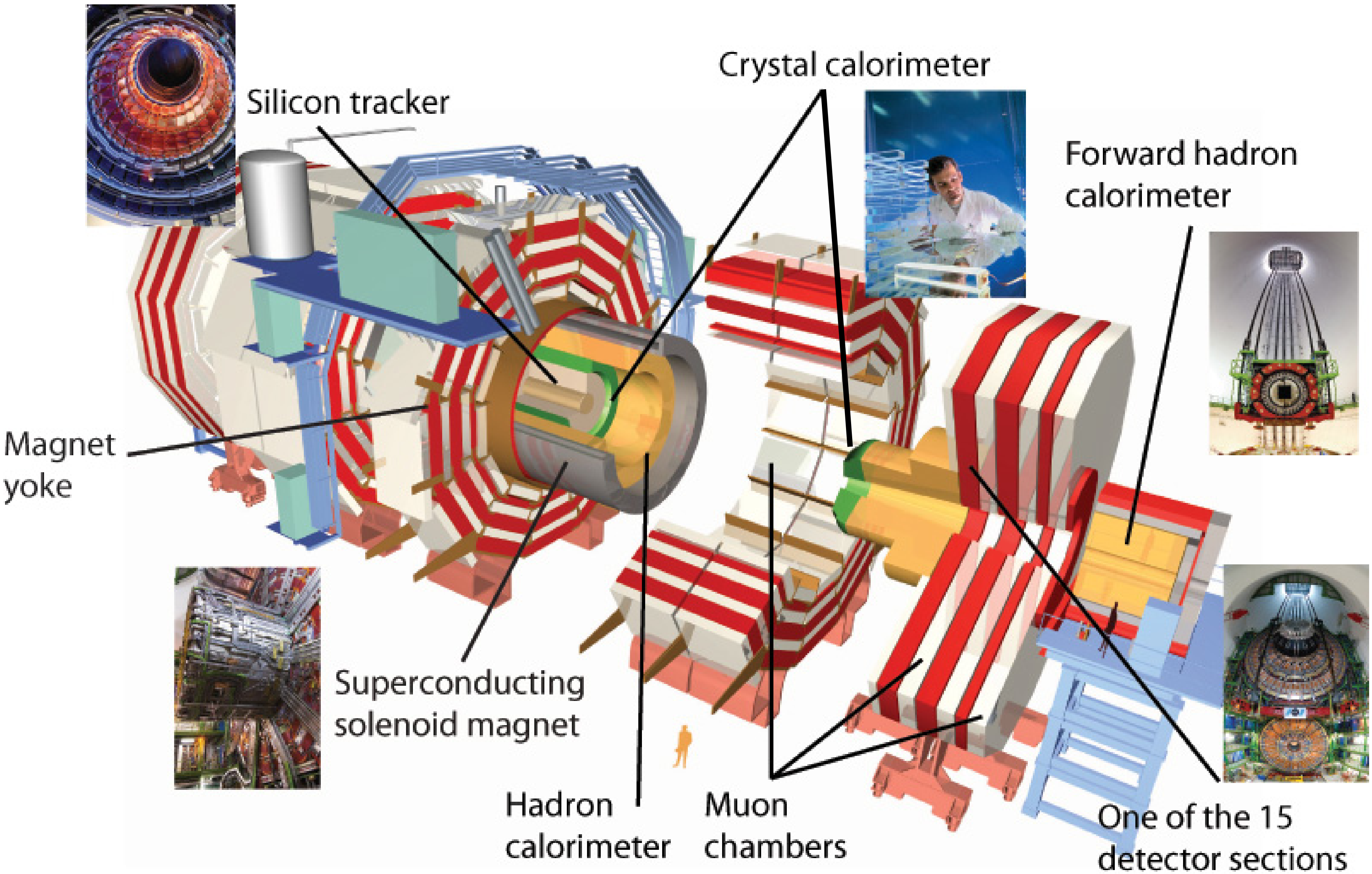

CMS crystal calorimeter ($PbWO_4$)

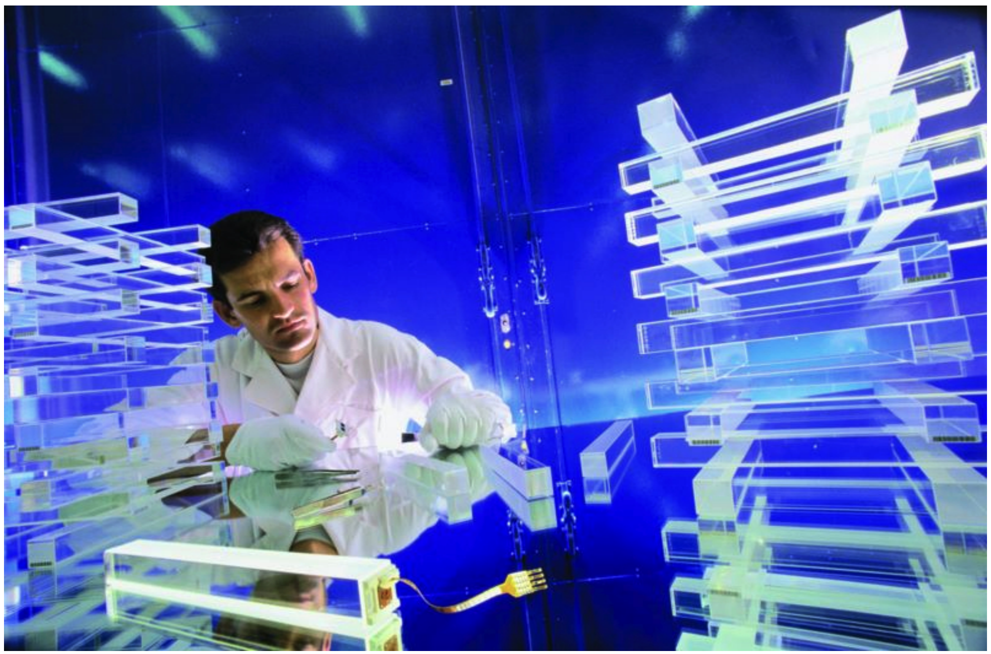

The crystals

End-cap electromagnetic calorimeter

Homogeneous calo: alternative to scintillators

DISADVANTAGE OF SCINTILLATING CRYSTALS: high costs and limitation in producing large volumes

Alternative: use Cherenkov radiator

Electrons and positrons of em shower emit Cherenkov light

- Number of photons is proportional to total path length of electrons and positrons: $N_{ph} \propto E_0$
- Resolution limited by photoelectron statistics (typical: about 1000 photo electrons per GeV shower energy)

Mostly used: lead glass, e.g. SF5: n=1.67, β_{thr}=0.6 or E_{thr}=0.62 MeV for electrons

Blocks of typical size 14 x 14 x 42 cm^3 $\rightarrow$ diameter 3.3 R_M and depth 17.5 X_0

Readout with photomultipliers.

Typical performance:

$$\frac{\sigma_E}{E} = 0.01 + 0.05\sqrt{E(\mathrm{GeV})}$$

Lead glass calorimeter

Lead glass blocks from the OPAL calorimeter

Now recycled in NA62 (photon veto)

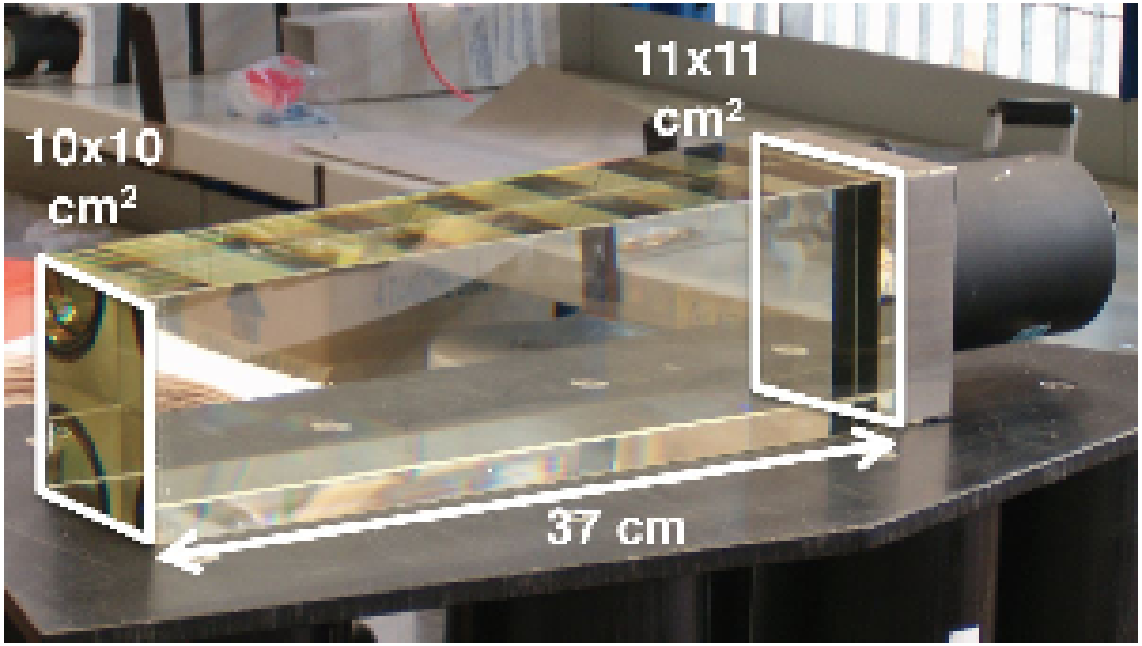

Sampling calorimeters

Signal generated in material different from material where the main energy loss occurs.

Shower (energy loss) only “sampled”

Simpler and more economical solution.

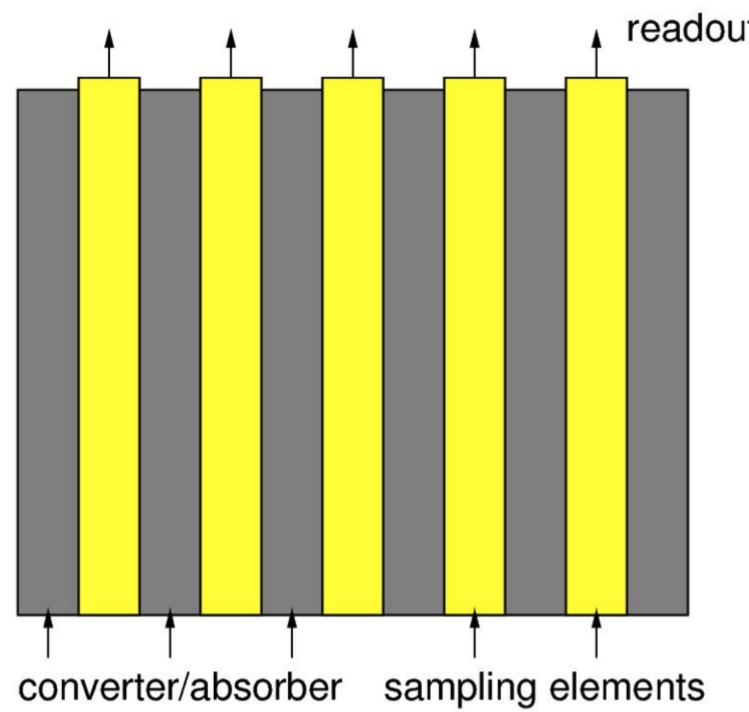

Converter medium:
Pb, W, U, Fe ← energy loss

Detection medium:
scintillator, liquid Ar ← sampling of shower

Longitudinal shower development: $t_{max} = t^{abs}_{max} \dfrac{x+y}{x}$

Transverse shower development: $R(95\%) = 2R_M \dfrac{x+y}{x}$

$x = \sum x_i$ absorber

$y = \sum y_i$ detection element

Energy loss in absorber and detection medium varies event-by-event

SAMPLING FLUCTUATIONS: additional contribution to energy resolution

Sampling calorimeters

History:

- 1954: N.L. Grigorov put forward idea of sampling calorimeters using proportional counters and scintillation counters between thick iron sheets to measure cosmic ray particles with E > 10^{14} eV
  - 1957: installation on Pamir mountains with 10m^2 of double layer of emulsions to study cosmic ray showers

1960-70's: particle experiments at accelerators

- 1965: C. Heusch and C. Prescott in CALTECH studied em shower development in plastic scintillators + lead absorbers, and lucite-based materials with lead absorbers
- 1973: H. Schopper and his group in Karlsruhe made studies with similar detectors for a hadronic calorimeter

Example: PHENIX PbScint calorimeter

Alternating layers of Pb sheets and plastic scintillator sheets connected to PMT via scintillating fibres

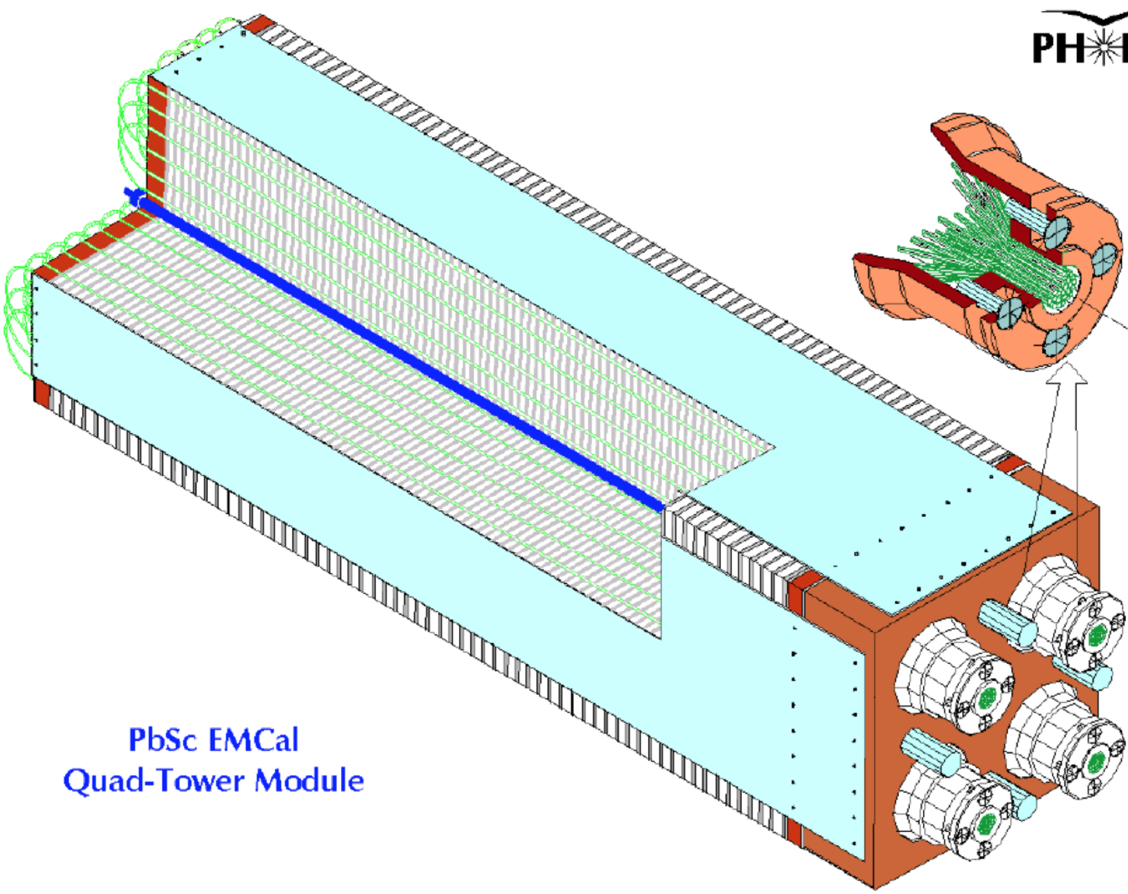

individual towers 5×5 cm^2

38 cm depth ($18X_0$)
66 sampling cells

in total covering 48 m^2
in 15552 individual towers

Parameter	Value
Lateral segmentation	5.535 x 5.535 cm^2
Active cells	66
Scintillator	4 mm Polystyrene
	(1.5% PT/0.01% POPOP)
Absorber	1.5 mm Pb
Cell thickness	5.6 mm (0.277 X_0)
Active depth	
(mm)	375 mm
(Rad. length)	18
(Abs. length)	0.85
WLS Fiber	1mm, BCF-99-29a
WLS fibers per tower	36
PMT type	FEU115 M, 30 mm
Photocathode	Sb-K-Na-Cs
Rise time (25% - 80%)	$\leq$ 5 ns

Example: PHENIX PbScint calorimeter

one module of PHENIX EMCal

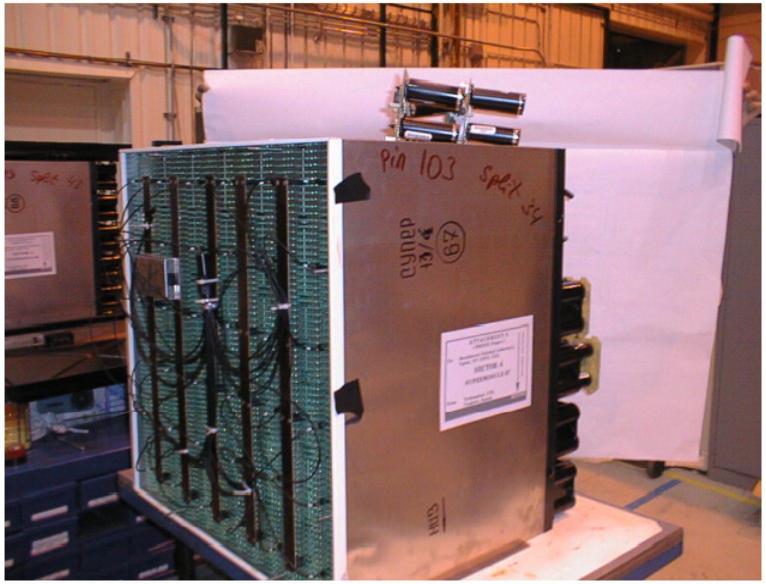

and entire WestArm

Example: PHENIX PbScint calorimeter

Nominal energy resolution: stochastic term: 8%/√E

Constant term: 2%

Time resolution: 200 ps

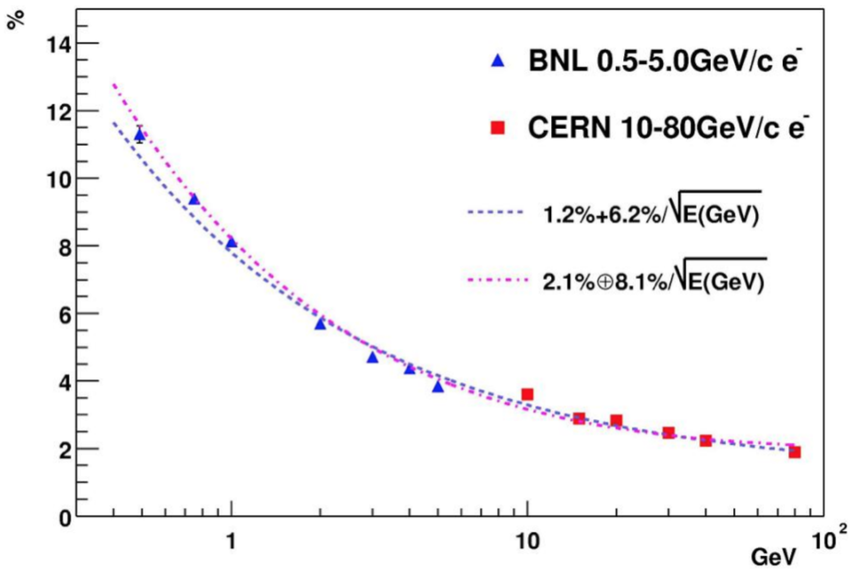

energy resolution

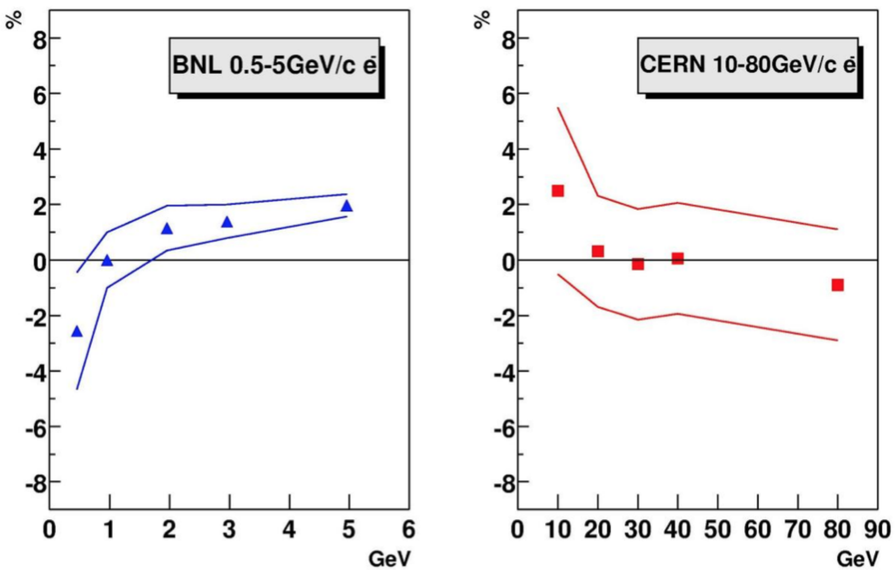

linearity of energy scale

Example: PHENIX PbScint calorimeter

Lateral shower profile well understood
→ position resolution in mm range

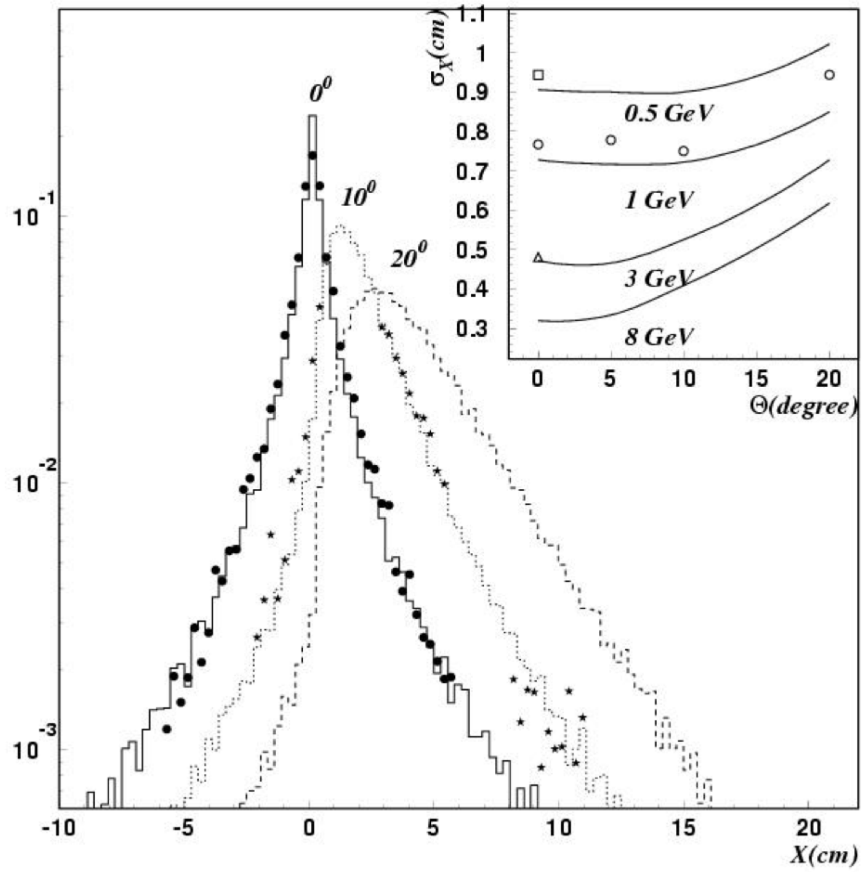

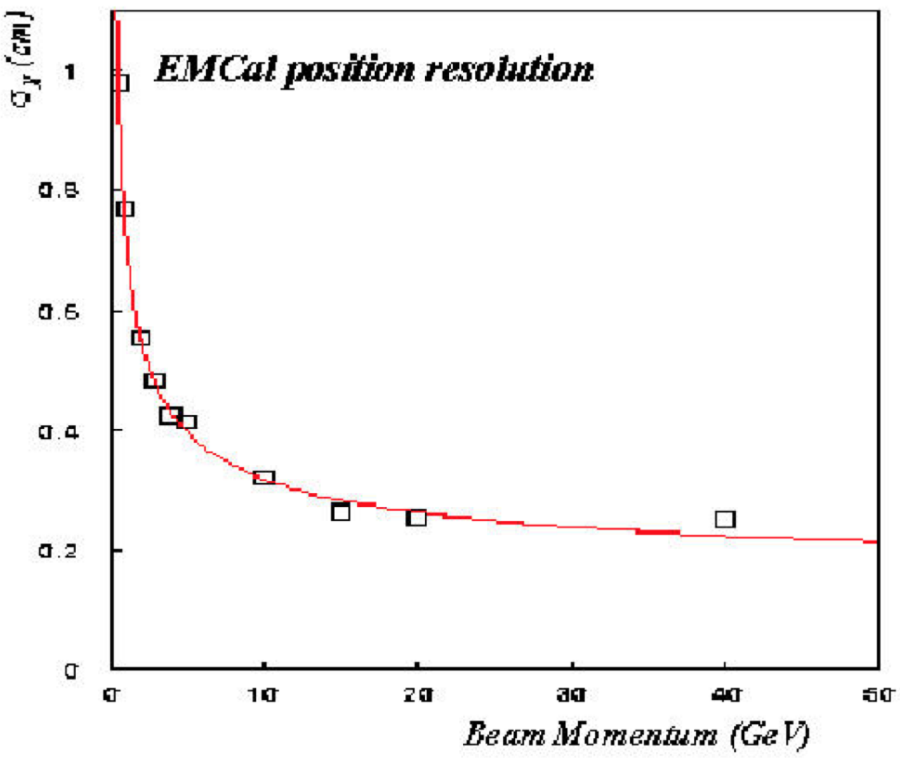

Liquid-argon sampling calorimeter

Alternative to scintillator and optical readout: use of liquid noble gas and operation of sampling sections as ionization chamber

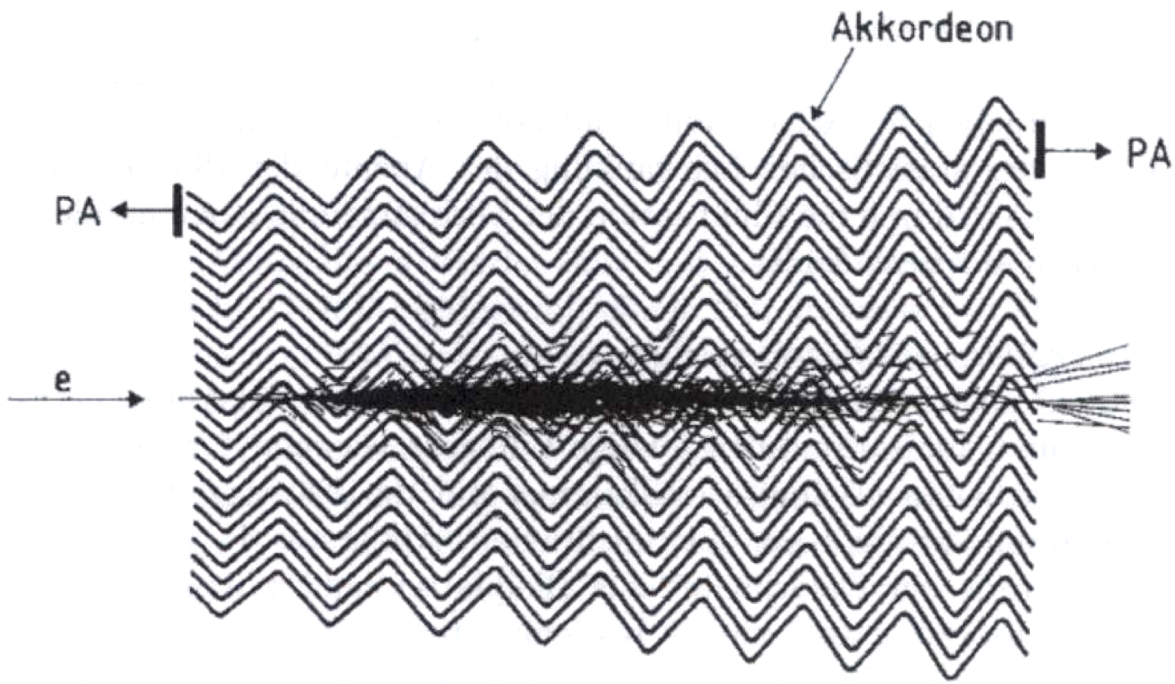

For faster readout: interleave electrodes between metal plates and electronics directly on electrodes inside liquid

Example: electromagnetic calorimeter of ATLAS

Outlook

At TeV energies we can also do muon calorimetry → they loose energy proportionally to their energy → stopping them becomes possible

Example: Future Circular Collider → muons with energy > 1 TeV

Calorimeters in a collider experiment: CMS

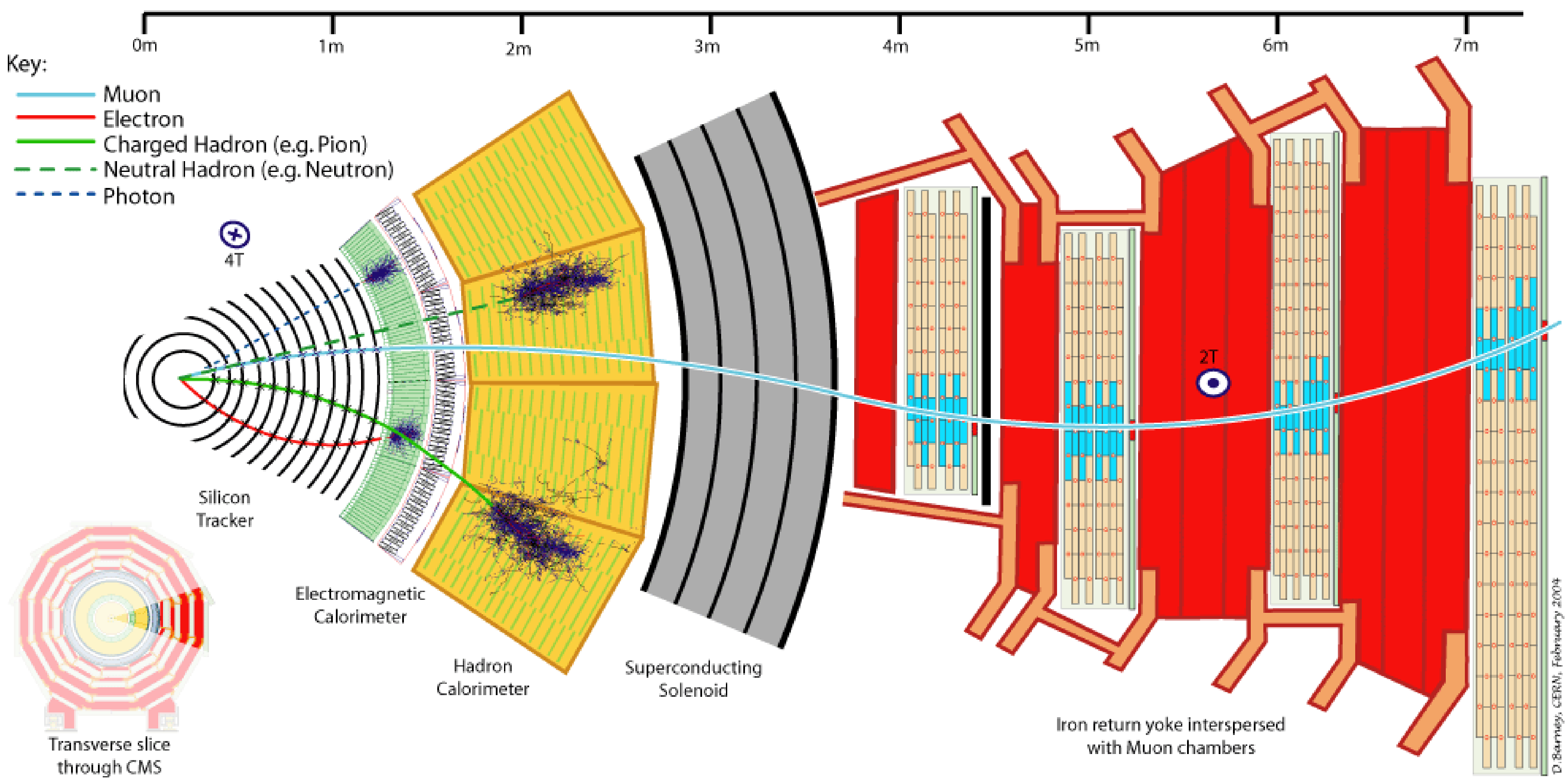

- Trackers
- Calorimeters
- Muon detectors

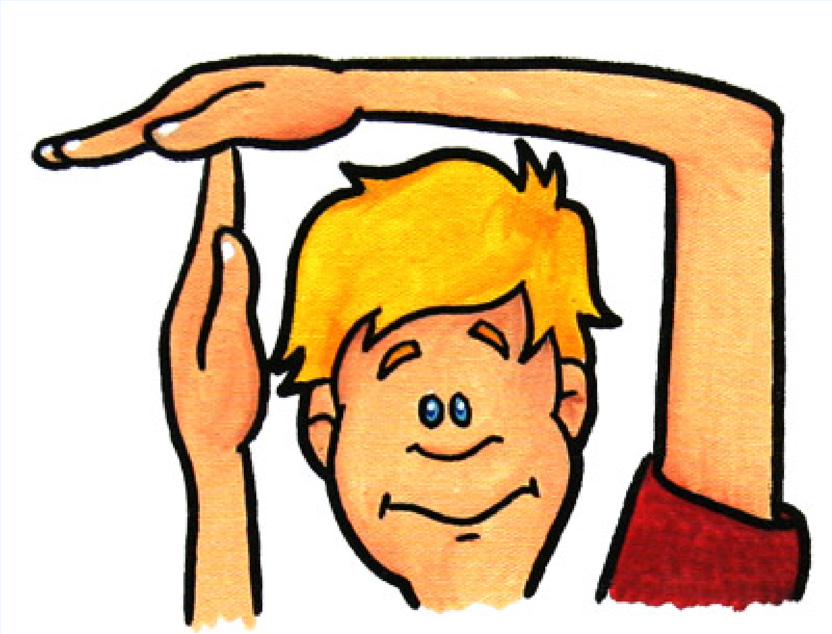

Hadronic calorimeters

Electromagnetic calorimeters - summary

Electrons, positrons, photons

- $E > E_c$
  - Bremsstrahlung
  - Pair production
- $E < E_c$
  - Electrons, positrons stopped within X_0
  - Photons need another 7-9 X_0

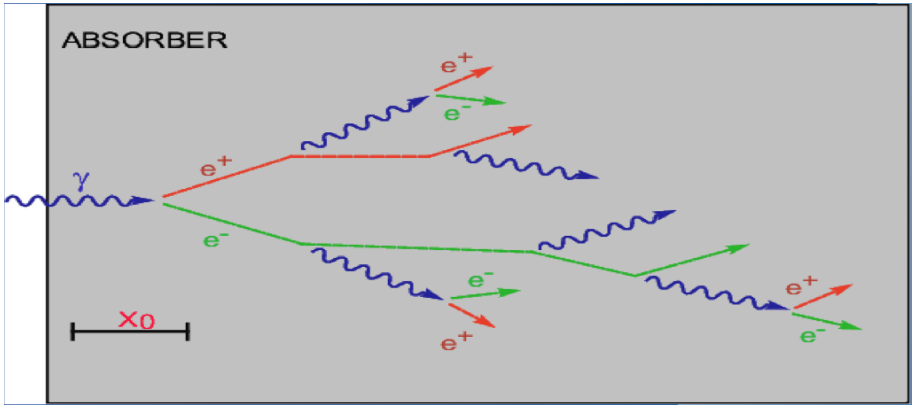

Longitudinal containment (95%): $t_{max} + 0.08\ Z + 9.6\ X_0$

Transverse containment (95%): 2 x Moliere radius

Energy leakage: mostly by soft photons escaping the calorimeter at the sides (later leakage) or at the back (rear leakage)

Showers: em and hadronic

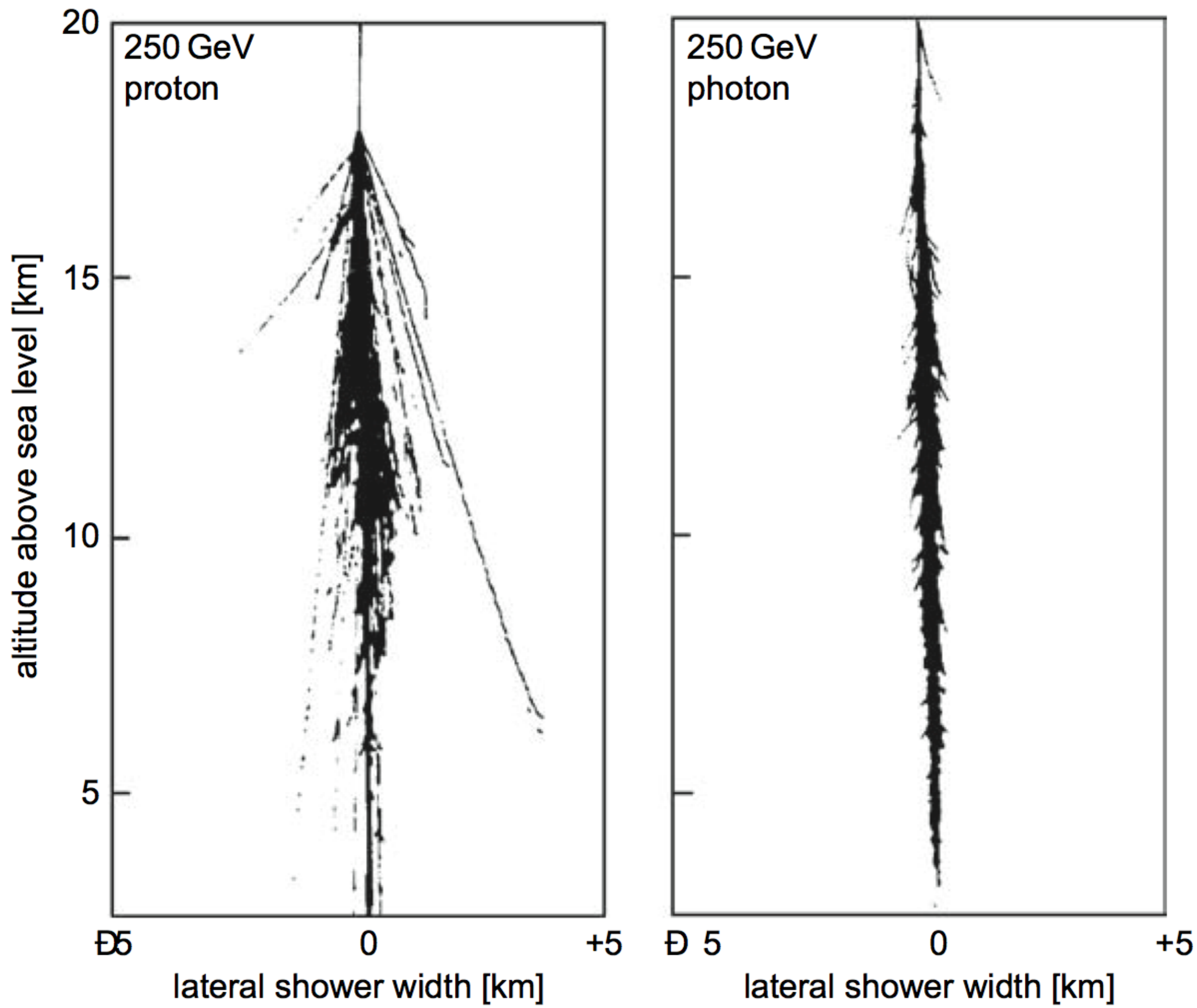

Fig. 8.16. Monte Carlo simulations of the different development of hadronic and electromagnetic cascades in the Earth's atmosphere, induced by 250 GeV protons and photons [51].

Hadronic calorimeters - outline

- **Hadronic showers**
  - Hadron interaction with matter
  - Shower development (longitudinal and lateral)
- **Hadronic calorimeters**
  - Sampling calorimeters
- **Compensation**
- **Particle identification**
- ATLAS hadronic calorimeters

Interaction of hadrons with matter

As reference, consider the interaction of protons (with E ≥ 1 GeV) with a nucleon (e.g. another p) or a nucleus:

Elastic	$p + N \rightarrow p + N$	σ_{el}
Inelastic	$p + N \rightarrow X$	σ_{inel}

$$\sigma_{tot} = \sigma_{el} + \sigma_{inel}$$

grows weakly with $\sqrt{s}$

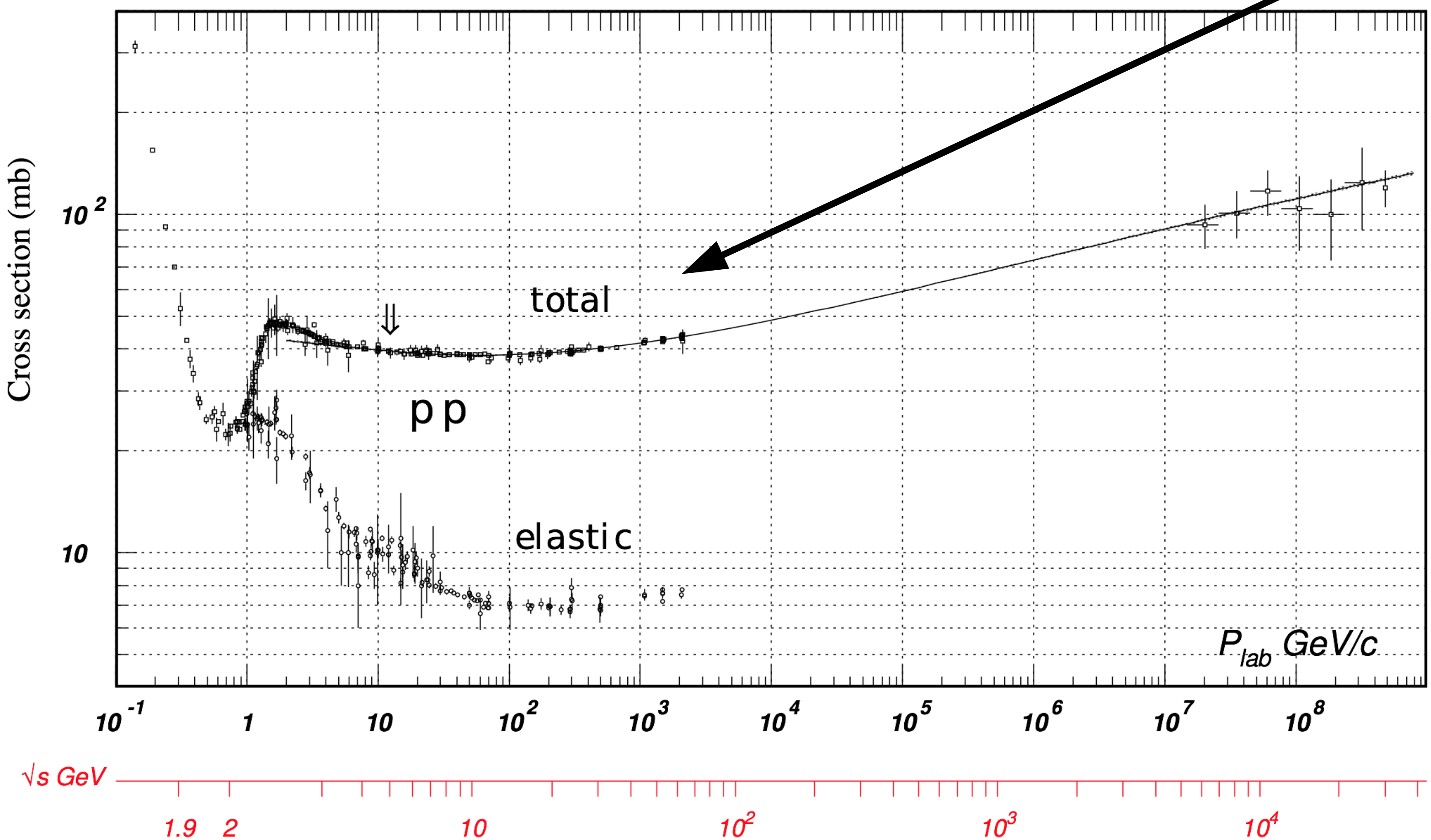

Interaction of hadrons with matter

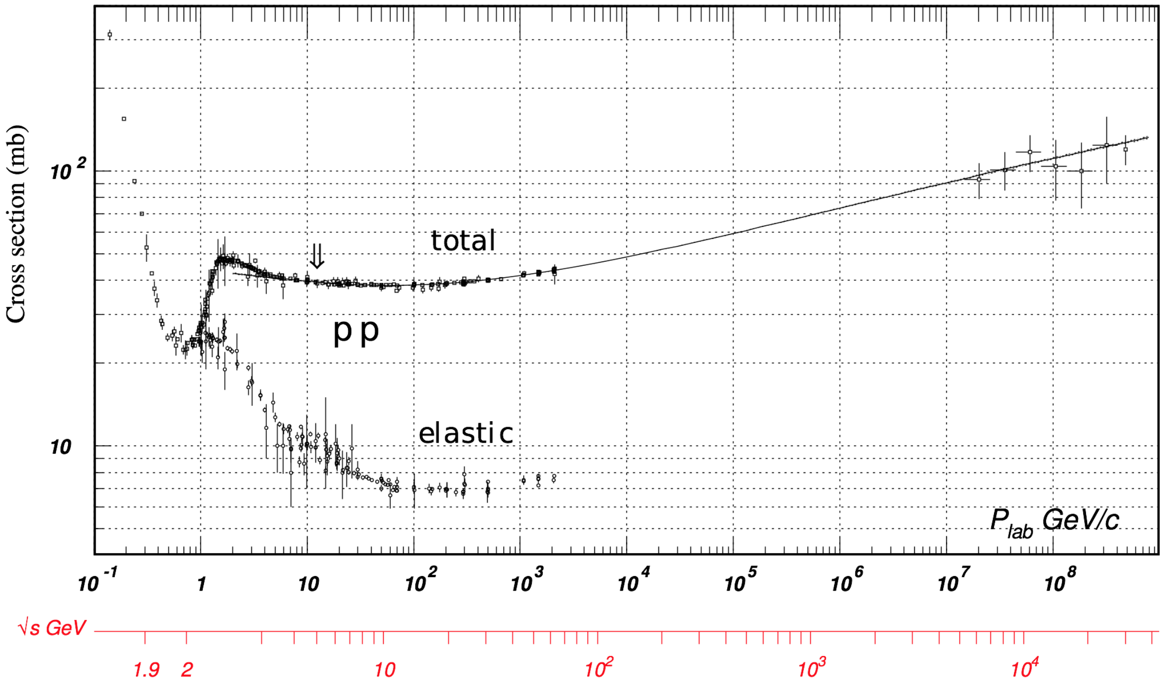

$\sqrt{s}$ (GeV)	σ_{tot} for pp (mb)
5	40
100	50
10000	100

- Elastic cross section ~ 10 mb
- At high energy there is also a diffractive contribution (similar to elastic)
- Majority of σ_{tot} is due to the **inelastic** component σ_{inel}

- Proton-nucleus: σ_{tot} (pA) $\simeq$ σ_{tot} (pp) · $A^{2/3}$

Hadronic interaction length

Average nuclear interaction length: $\lambda_W = \dfrac{A}{N_A \rho \sigma_{tot}}$

For inelastic processes → absorption: $\lambda_A = \dfrac{A}{N_A \rho \sigma_{inel}}$

$$N(x) = N_0 \exp\left(-\frac{x}{\lambda_A}\right)$$

$$\lambda_A \simeq 35 \frac{g}{cm^2} \cdot A^{\frac{1}{3}} \quad \text{for } Z \geqslant 15 \text{ and } \sqrt{s} \simeq 1-100\,\text{GeV}$$

	C	Ar (lq)	Fe	U	scint.
λ_A (cm)	38.8	85.7	16.8	11.0	79.5
X_0 (cm)	19.3	14.0	1.76	0.32	42.4

$\lambda_A \gg X_0$!!

→ hadronic calorimeters are larger (“thicker”) than electromagnetic ones

For 95% containment:
Typical longitudinal size: 9 λ_A
Typical transverse size: 1 λ_A

Hadronic shower

- p + nucleus → $\pi^+ + \pi^- + \pi^0$ .... + nucleus*
  ↳ nucleus 1 + n, p, α
  ↳ nucleus 2 + 5 p,n
  ↳ fission
- Secondary particles undergo further inelastic collisions with similar cross sections, until they fall below the pion production threshold
- Sequential decays:
  - $\pi^0 \rightarrow \gamma\gamma \rightarrow$ electromagnetic shower
  - Fission fragments → β-decay, γ-decay
  - Nuclear spallation: individual nucleons knocked-out of nucleus, de-excitation
  - Neutron capture → nucleus* → fission (U)

At every "step" about 1/3 of deposited energy goes into em shower

- Mean number of secondary particles $\propto \ln E$. Typical transverse momentum $\langle p_T \rangle \sim 350$ MeV/c
- Mean inelasticity (fraction of E in secondary particles) ≃ 50%

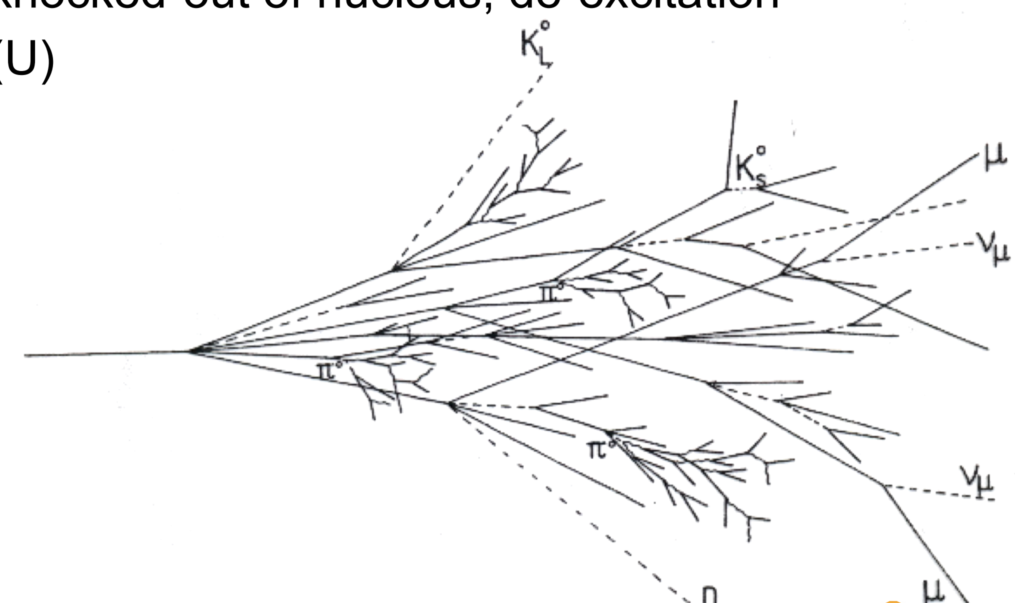

Shower development

Extremely rough analytic description (**fluctuations are huge**):

Similarly to em showers, but important differences!!!

Variable: $t = x/\lambda_A$ depth in units of interaction length

E_{thr} = 290 MeV (diff!)

$$E(t) = \frac{E}{\langle n \rangle^t}$$

$$E(t_{max}) = E_{thr} \quad \rightarrow \quad E_{thr} = \frac{E}{\langle n \rangle^{t_{max}}}$$

$$\langle n \rangle^{t_{max}} = \frac{E}{E_{thr}} \quad \text{or} \quad t_{max} = \frac{\ln E/E_{thr}}{\ln \langle n \rangle}$$

Compared to em shower:

- Number of particles in hadronic shower lower by a factor E_{thr}/E_c
- Intrinsic resolution worse by factor $\sqrt{E_{thr}/E_c}$

Shower development

Significant variations and fluctuations of the energy sharing!!

- Part of energy is invisible

  Neutron capture leads to fission → release of binding energy
- Variation in SPATIAL distribution of energy deposition ($\pi^{\pm} \leftrightarrow \pi^0$)
- Electromagnetic fraction grows with E: $f_{em} \simeq f_{\pi 0} \propto \ln[E(\mathrm{GeV})]$
- Energetic hadrons contribute to electromagnetic fraction by e.g. $\pi + p \rightarrow \pi^0 + n$, but very rarely the opposite happens (a 1 GeV π^0 travels 0.2 μm before it decays)
- Below pion production threshold, mainly dE/dx by ionization

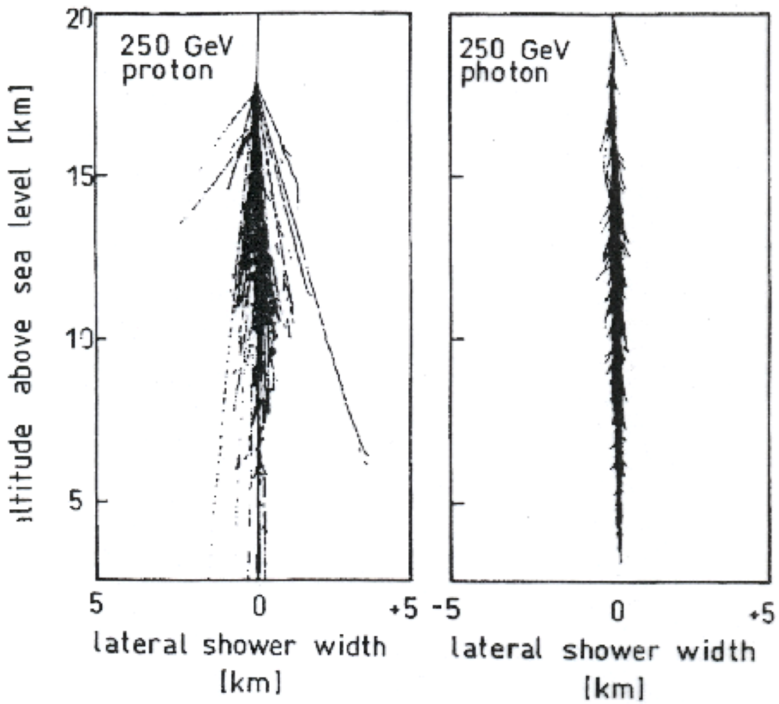

Monte-Carlo simulated air showers

Shower development

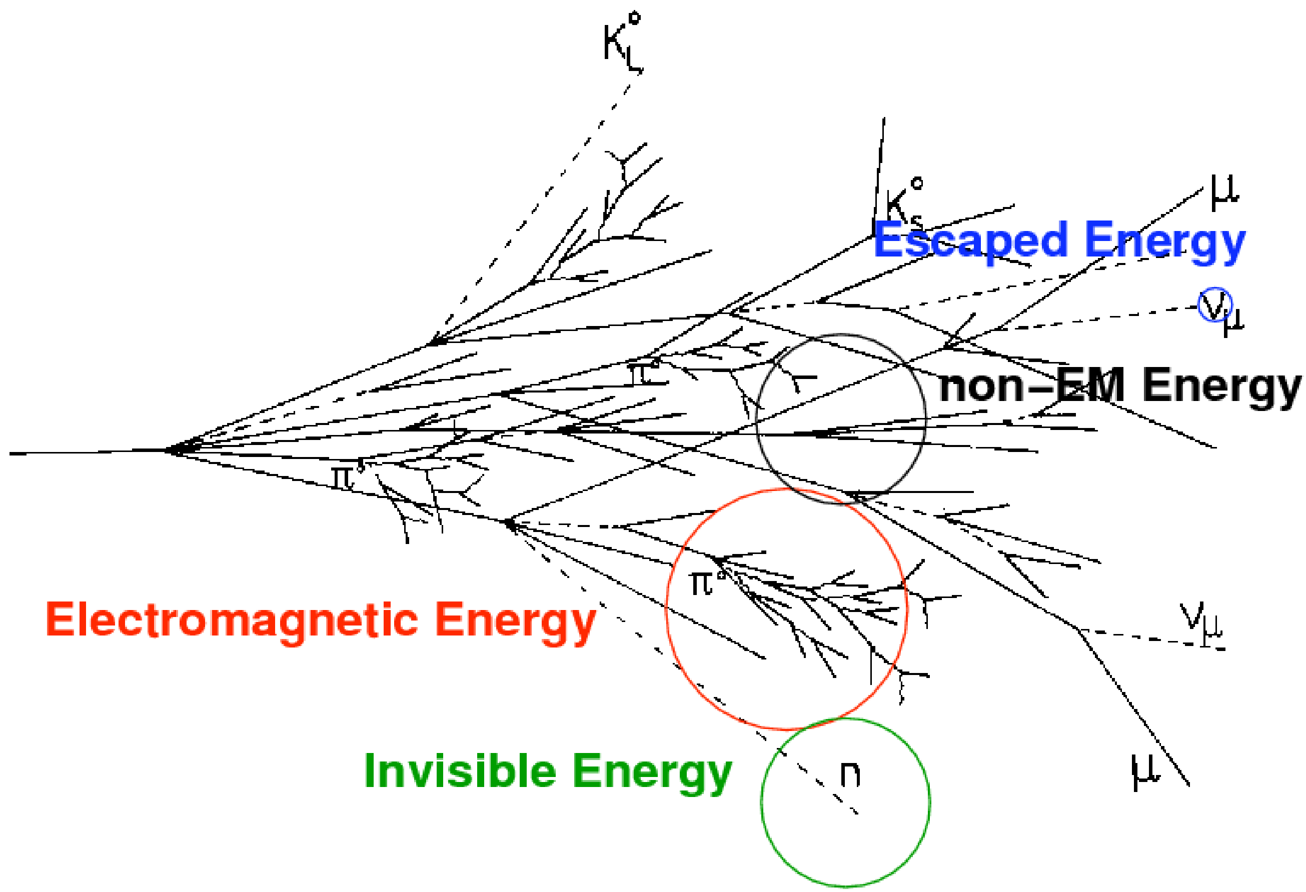

Shower development

Deposition of energy:

- Electromagnetic fraction (e, π^0, η^0) ~ 30%
  however π^0 production is subject to large fluctuations!

- Ionization energy by charged hadrons (p,π,K) up to 40%

- Invisible fraction of energy ~ 30 – 40 %
  - Hadrons break up nuclear bonds
    → nuclear binding energy
    → short-range nuclear fragments mostly absorbed before detector layers
  - Long-lived or stable neutral particles escape: neutrons, K^0_L, neutrinos
  - Muons created as decay products of pions and kaons deposit very little part of their energy

Because of the invisible energy fraction and the large fluctuations, the energy resolution is significantly worse compared to the em case

Shower development

Shower simulations via intra- and inter-nuclear cascade models
(e.g. GEISHA, CALOR, etc)

Common features, but significant variations! Need to tune to measured data

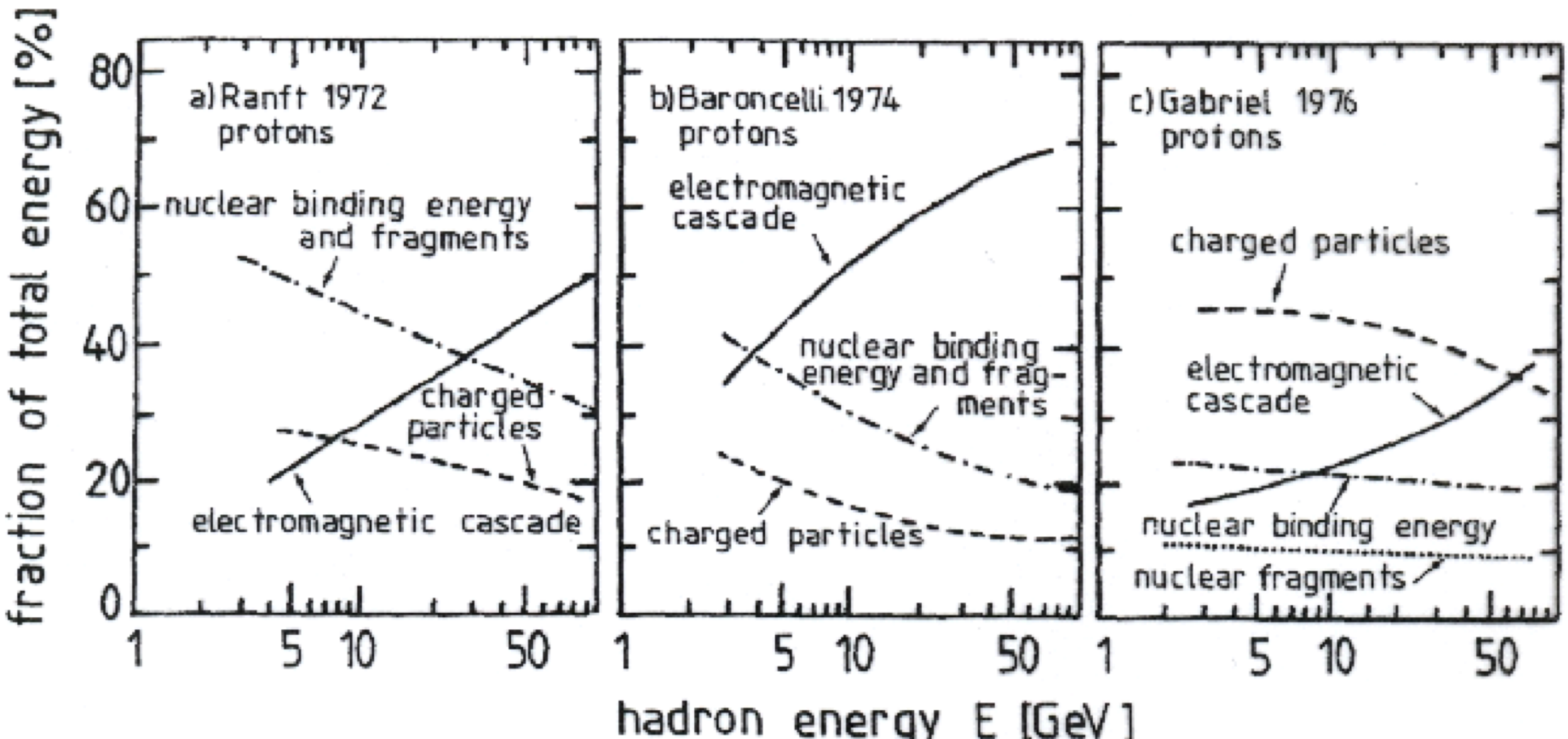

Longitudinal shower development

- Strong peak near hadronic interaction length
- Followed by exponential decrease
- Shower depth:

  $t_{max} \simeq 0.2 \ln E(\text{GeV}) + 0.7$

  95% of energy in $L_{95} = t_{max} + \lambda_{att}$

  where $\lambda_{att} \simeq E^{0.3}$ (E in GeV, λ_{att} in units of λ_A)

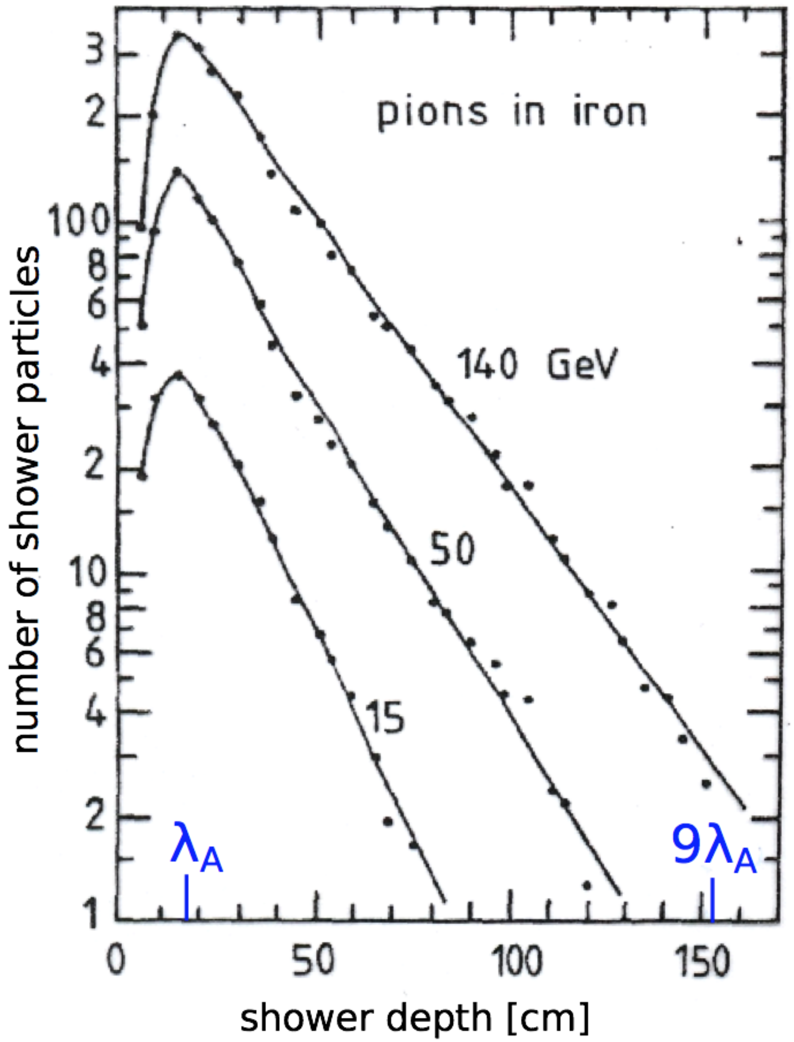

Example: 350 GeV $\pi^{\pm}$

$t_{max} = 1.9$ $L_{95} = 1.9 + 5.8$

Need about 8 λ_A to contain 95% of energy

Need about 11 λ_A to contain 99% of energy

Lateral shower development

- Typical transverse momentum for secondary hadrons $<p_T>$ ~ 350 MeV/c
- Lateral extent at shower maximum $R_{95} \simeq \lambda_A$ (sizably larger than em!!)
- Relatively well defined core with $R \simeq R_M$ (electromagnetic component) + exponential decay (hadronic component with large transverse momentum transfers in nuclear interactions)

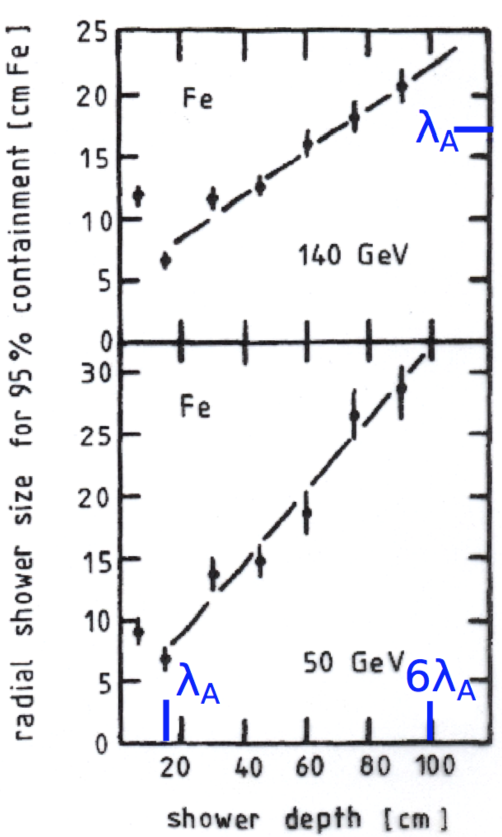

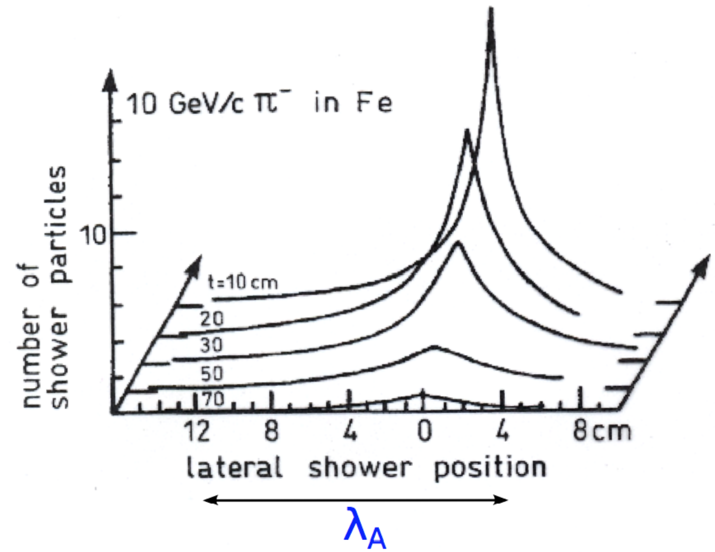

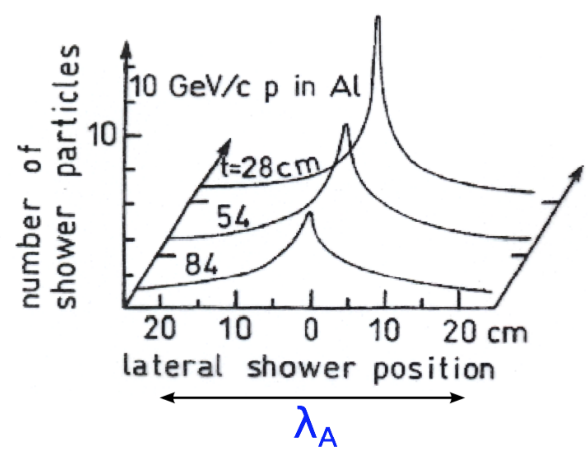

Hadronic calorimeters

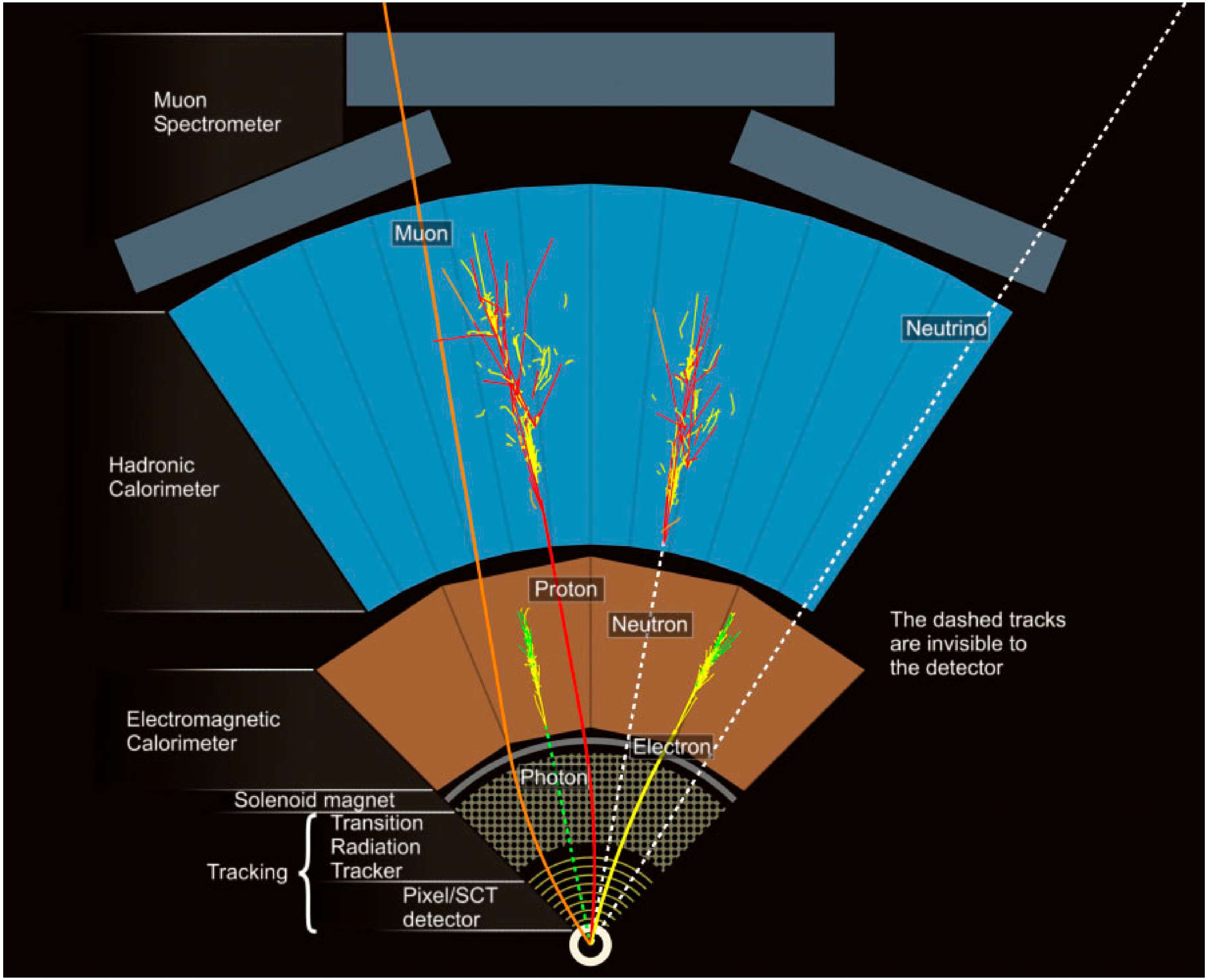

Hadronic calorimeters

Homogeneous calorimeter that could measure entire visible energy loss generally would be too large and expensive to realize. In all cases fluctuations of invisible component make this expense not worth.

→ most common: **sampling calorimeters!**

- Alternating layers of passive absorber (Fe, Pb, U) + sampling elements (scintillator, liquid Ar or Xe, MPWCs, layers of proportional tubes, streamer tubes, Geiger-Mueller tubes, ..)
- Also spaghetti or shish kebab calorimeter: absorber with scintillating fibers embedded

Hadronic calorimeters

Frequently electron and hadron calorimeters are integrated in a single detector. Here: iron-scintillator calorimeter with separate wavelength-shifter readout for electrons and for hadrons (two components can be separated)

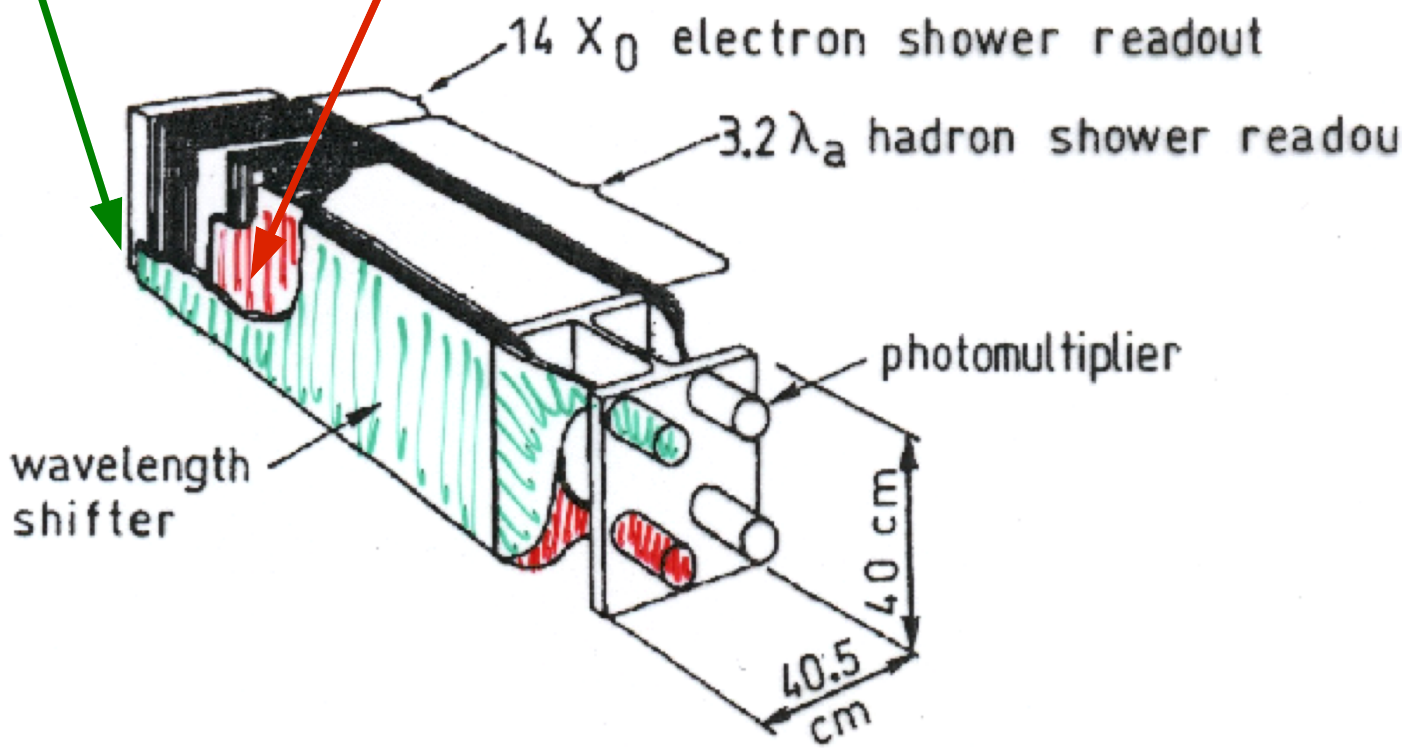

Energy resolution

- Intrinsic contributions
  - Leakage and its fluctuations
  - Fluctuations of electromagnetic portion
  - Heavily ionizing particles with $dE/dx \gg (dE/dx)_{\text{min.ion.}} \rightarrow$ saturation

  all scale like $1/\sqrt{E}$ as statistical processes

- Sampling fluctuations
  - Dominate in em calorimeter, are nearly completely negligible in hadronic ones: d_{abs} = thickness of one absorber layer

$$\sigma_{\text{sample}}/S \propto \sqrt{d_{abs}/E}$$

- Other contributions:
  - Noise: $\sigma_E/E = C/E$
  - Inhomogeneities: σ_E/E = constant

Add in quadrature:

$$\boxed{\frac{\sigma_E}{E} = \frac{A}{\sqrt{E}} \oplus B \oplus \frac{C}{E}}$$

A: 0.5 – 1.0 (record 0.35)
B: 0.03 – 0.05
C: 0.01 – 0.02

Quality of a calorimeter

… is based on the following criteria:

Limitations imposed by the complicated structure of the hadronic shower, with its very large fluctuations

- Linear response: signal $\propto$ E

  often linearity is not over large range

- Energy resolution $$\frac{\sigma_E}{E} = \frac{\text{const}}{\sqrt{E}}$$

  fluctuations make things deviate from optimal resolution

- Signal independent from particle species

  response to electromagnetic and hadronic components can be very different relative to each other → e/h issue

e/h (or e/π) issue → compensation

Generally the response to electromagnetic and hadronic energy deposition is different!

Usually the electromagnetic component has higher weight, since the hadronic shower has an invisible component → **e / h > 1 !!!** **(*)**

This is a serious limitation to the measurement of the total energy flow in an event!

Optimization:

"Compensation"

"Overcompensation" (e / h < 1)

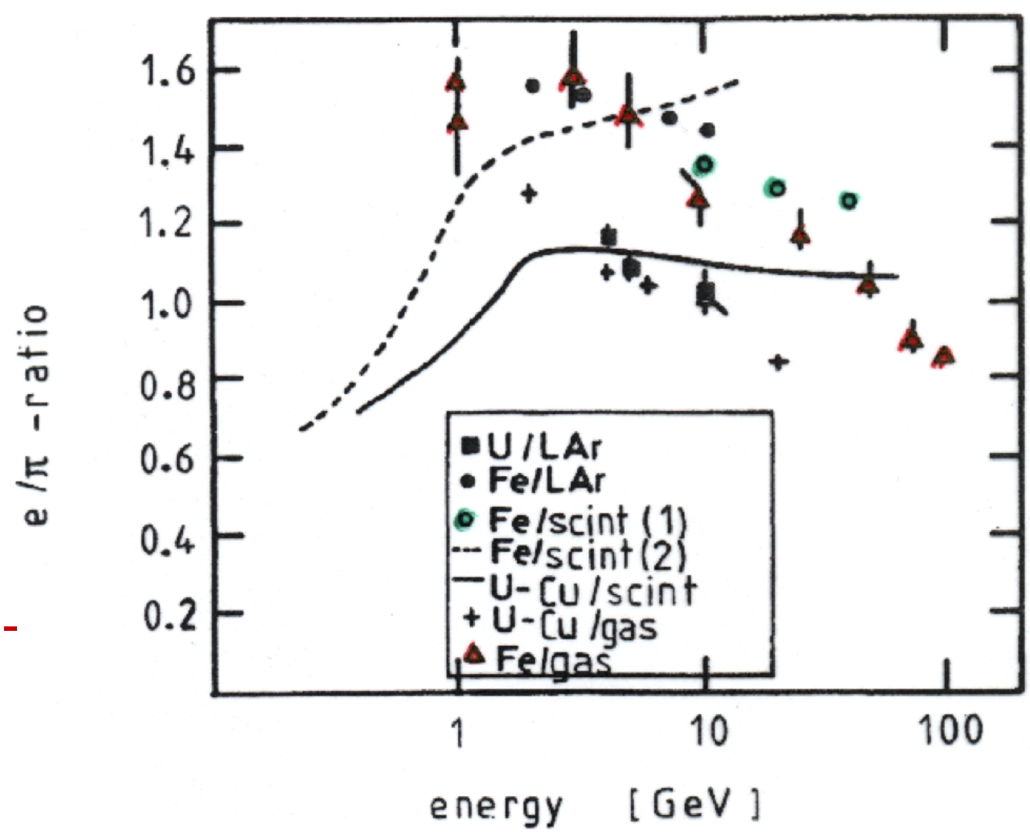

(*) ratio of energy deposits of an electron-initiated shower compared to that of a hadron-initiated shower for the same initial energy of electrons and hadrons

Software compensation

Consider the layers of active components of the calorimeter:

- Identify the layers with particularly large Ev → π^0 contribution
- Assign SMALL WEIGHT to these layers!

$w_i^* = w_i\,(1 - cw_i)$ $\quad$ w_i = measured, deposited energy

c = weight factor

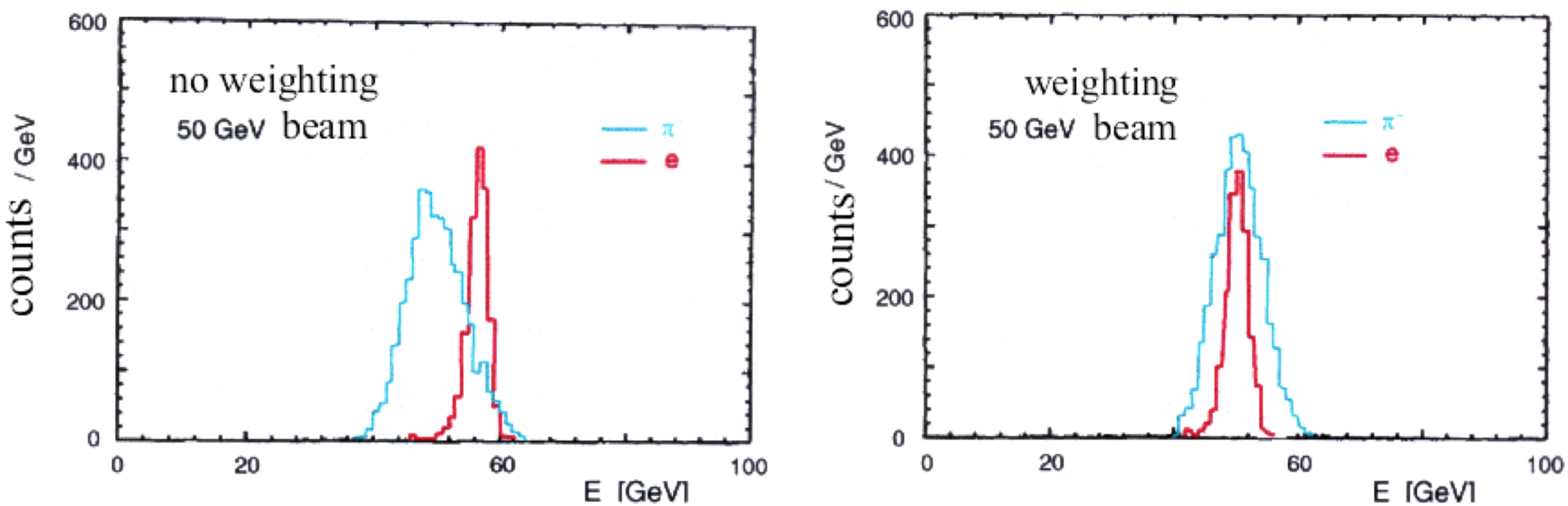

Hardware compensation

Essential if one wants to trigger!

Increase of h/mip or decrease of e/mip. Possibilities:

- Increase of hadronic response via fission and spallation of ^{238}U

  $\rightarrow$ increase of $\dfrac{\text{ion}}{\text{mip}}$ or $\dfrac{\text{n}}{\text{mip}}$

- Increase of neutron detection efficiency in active material: high proton content

  $Z=1 \rightarrow$ increase of $\dfrac{\text{n}}{\text{mip}}$

- Reduction of e/mip via high Z absorber and suitable choice of $\dfrac{d_{abs}}{d_{act}}$

  increase of $Z_{abs} \rightarrow$ decrease of $\dfrac{\text{e}}{\text{mip}} \leftarrow$ increase of d_{abs}

- Long integration time $\rightarrow$ sensitivity to γ capture after neutron thermalization

  $\rightarrow$ t long $\rightarrow$ increase of $\dfrac{\text{n}}{\text{mip}}$

Hardware compensation

calorimeter response to protons

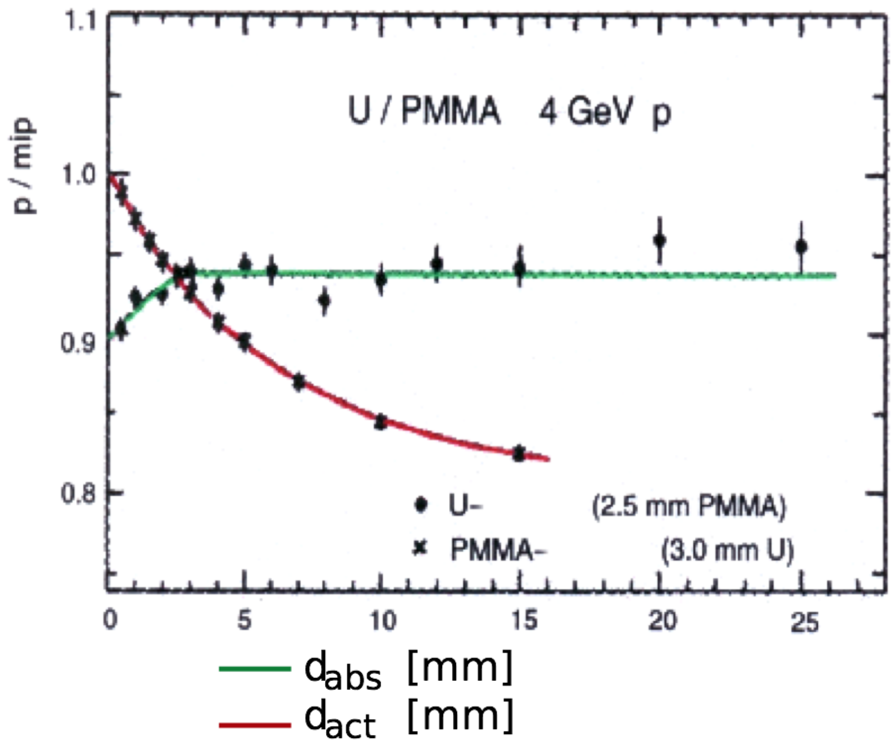

variation of plate thickness ↔ variation of response p/mip

calorimeter response to neutrons

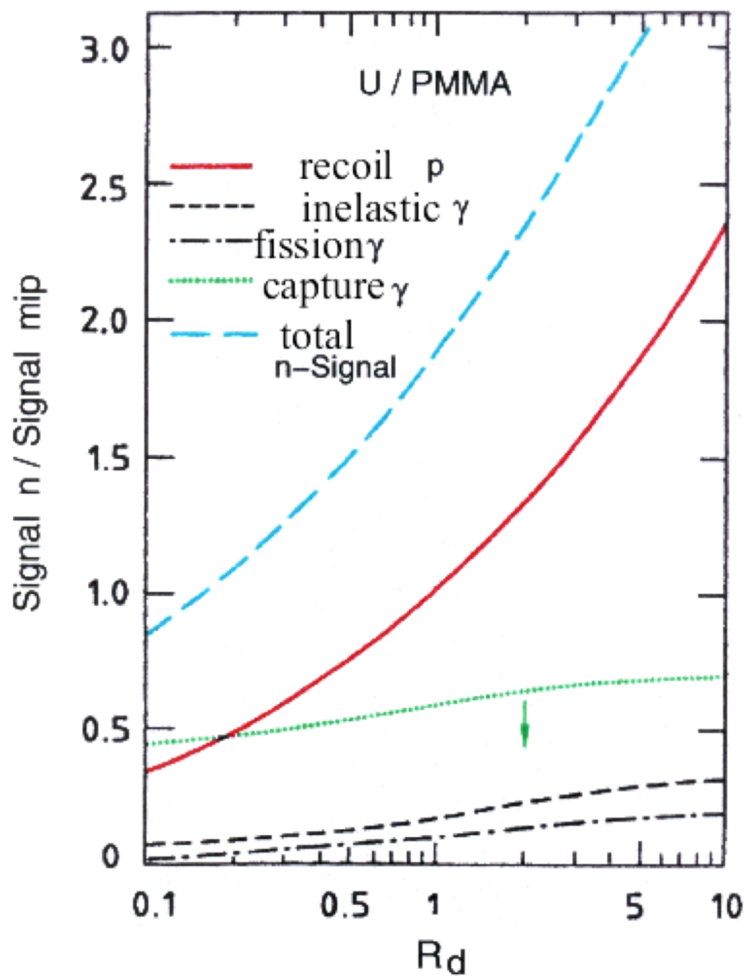

variation of contributions vs. $R_d = d_{abs}/d_{act}$

Time structure of showers

In em showers, all components cross the detector within few ns (speed ~ 30 cm/ns)

In hadronic showers, the component due to neutrons is delayed: they need to slow down before they produce a visible signal

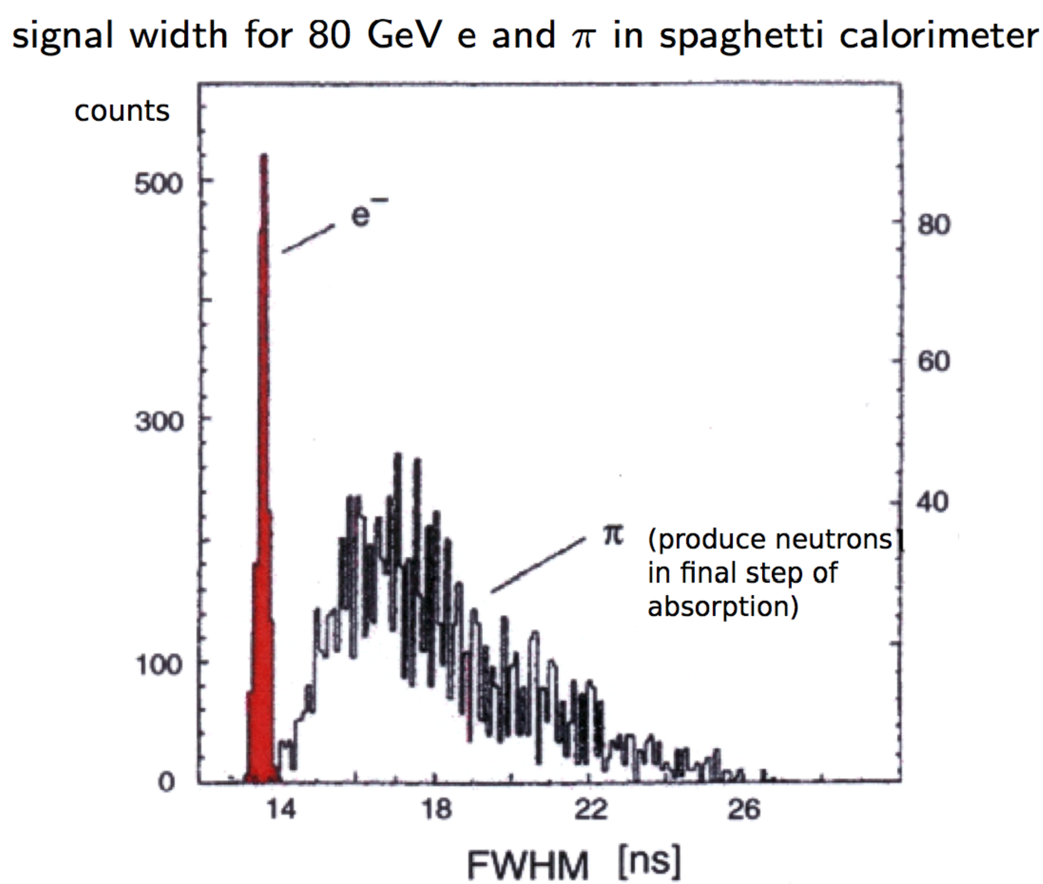

Size of signal depends on integration time → a variation of the integration time of the electronics can enhance the hadronic signal (used in the ZEUS calorimeter)

ZEUS calorimeter

U (3 mm) + Scintillator (2.5 mm)

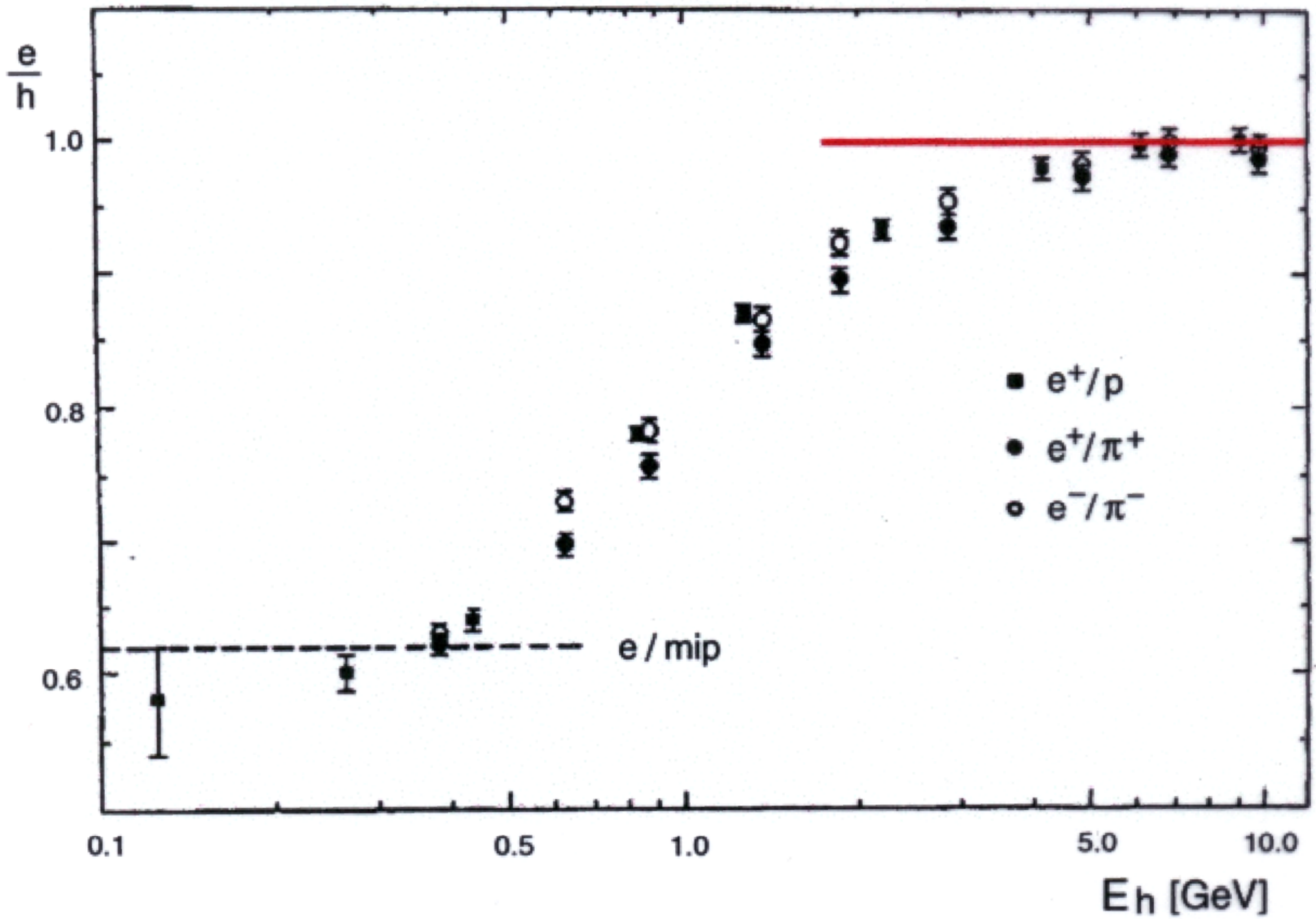

measured ratio of electron/pion signals at (ZEUS) for $E \geq 3$ GeV nearly compensated

Particle identification: e / π

Electron/pion: hadron showers are deeper and wider and start later!

- Difference in transverse and longitudinal shower extent
- Signal for electron is faster

→ PID based on likelihood analysis

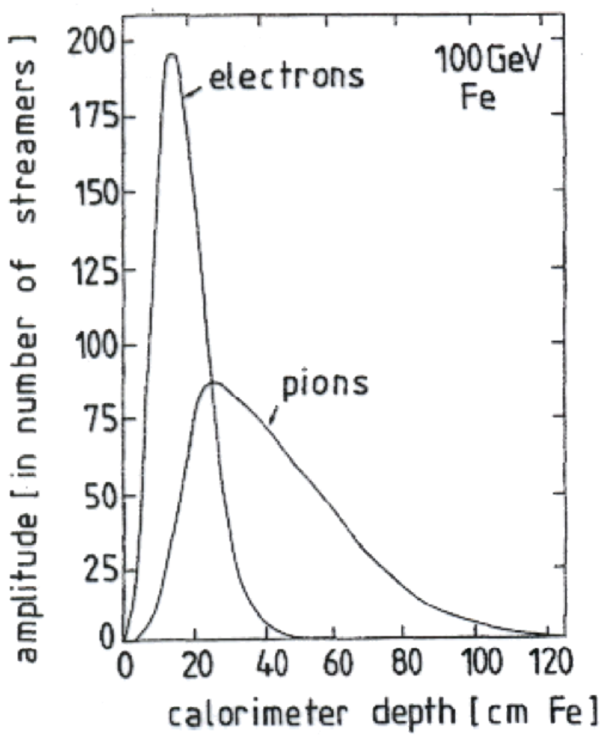

streamer tube calorimeter

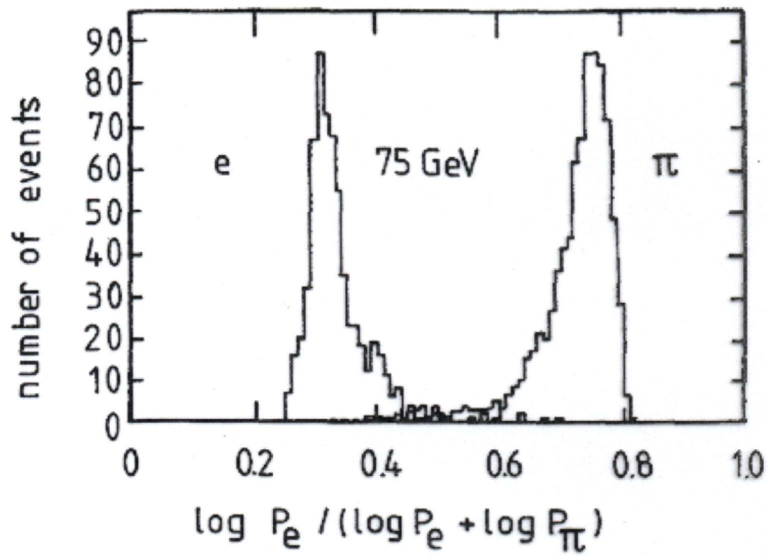

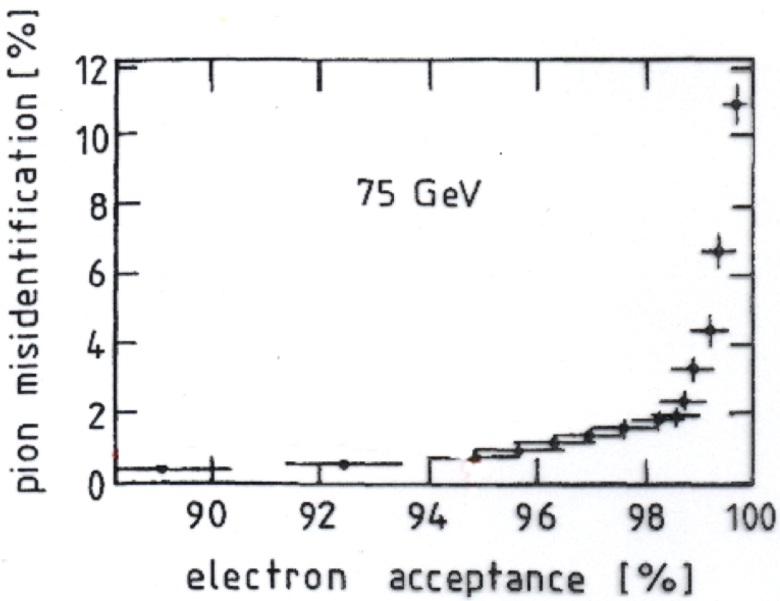

Particle identification: μ / e

low energy loss for muon

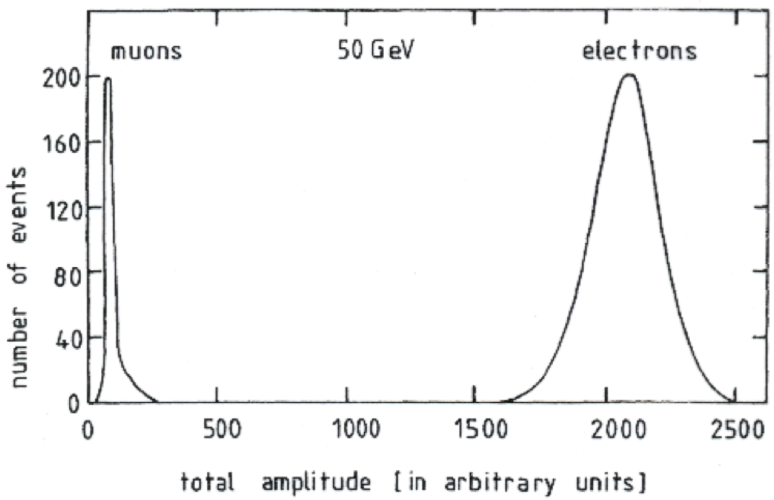

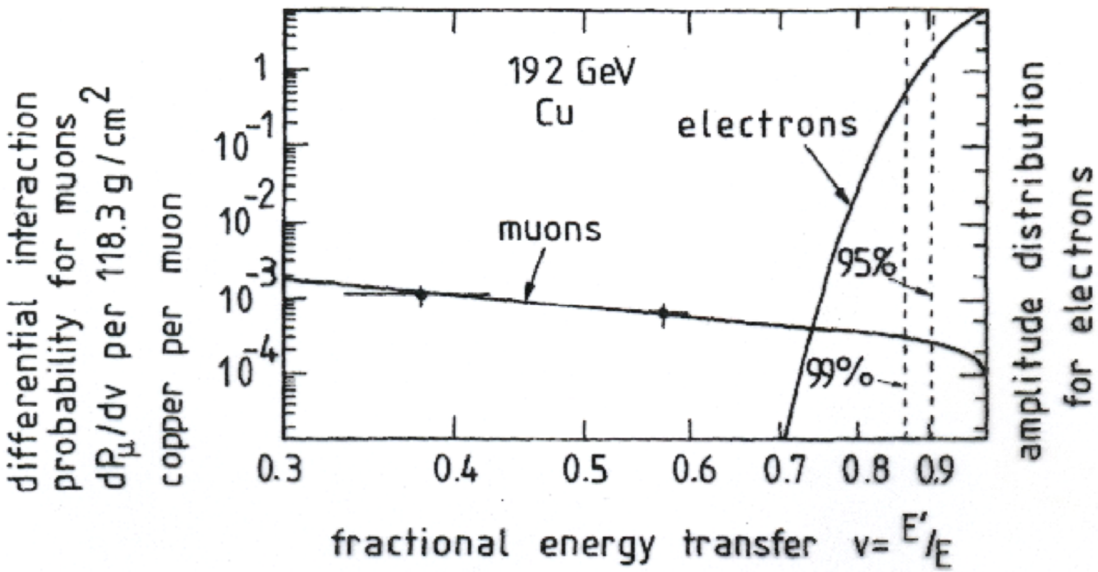

for 95% electron efficiency muon probability $1.7 \cdot 10^{-5}$

ATLAS hadronic calorimeters

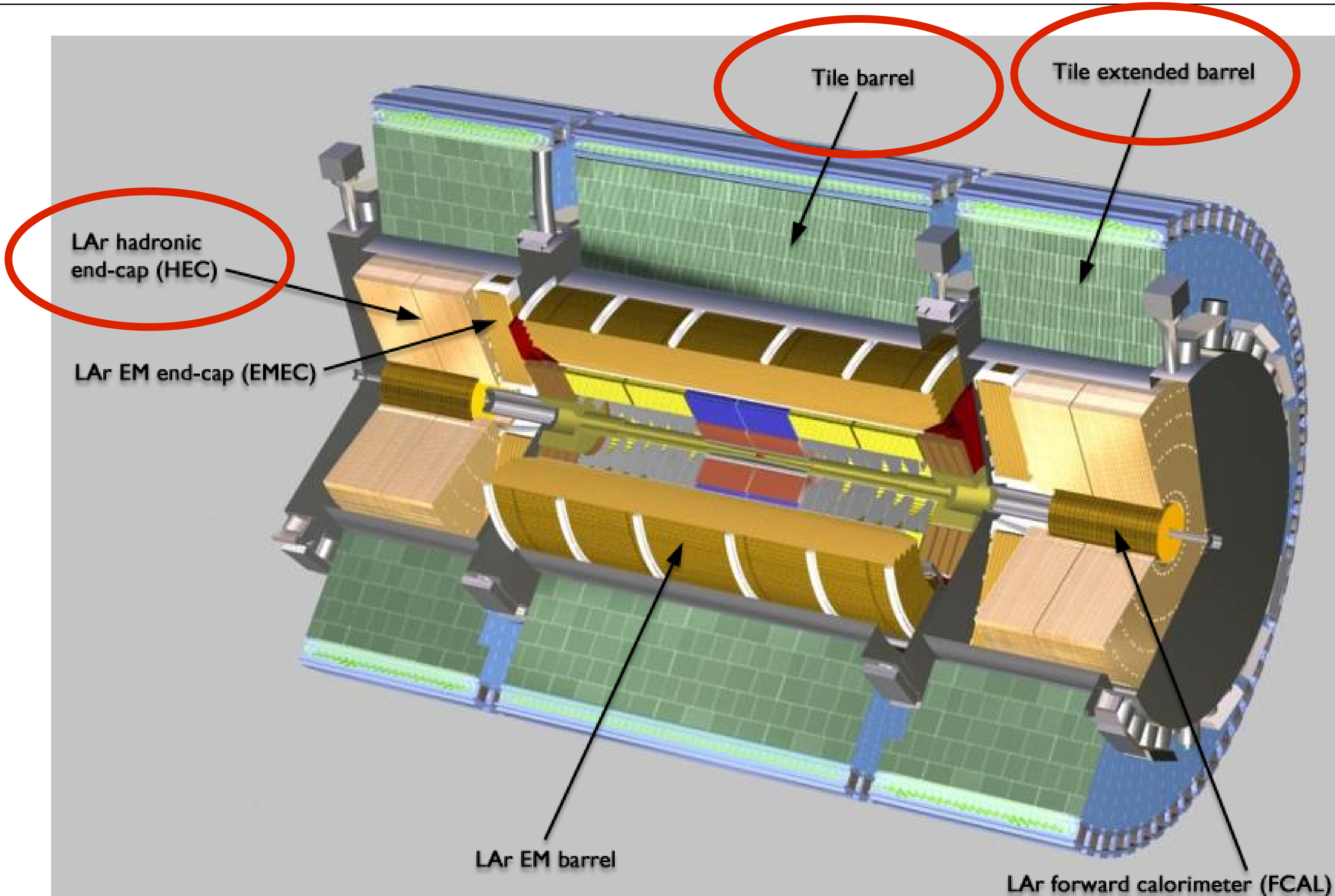

ATLAS hadronic calorimeters

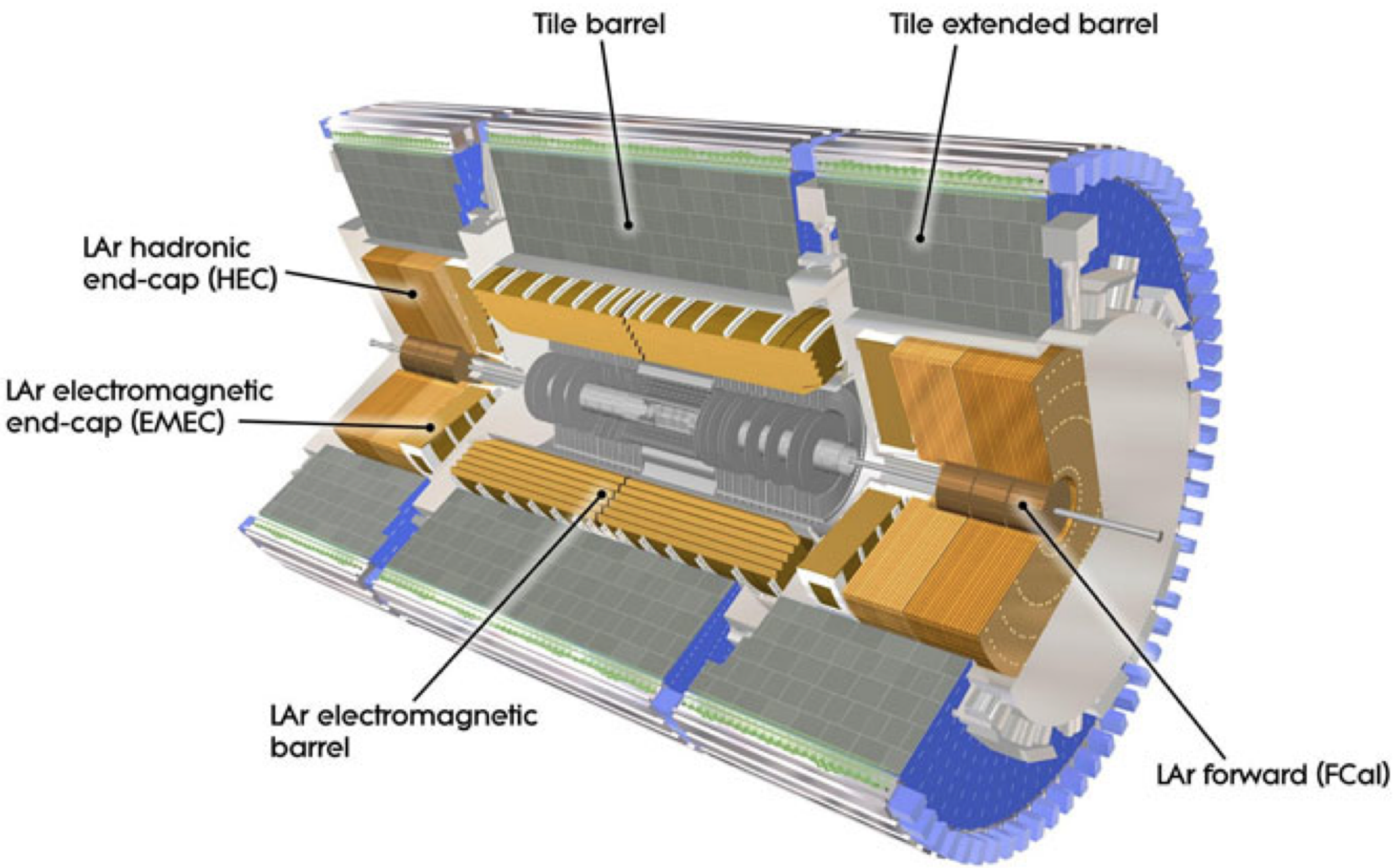

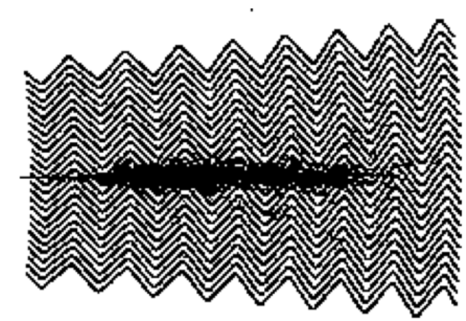

accordion-shaped layers of Pb absorber in liquid Ar as sensitive material (ionization measured in intermediate electrodes)

hadronic tile calorimeters:
steel sheets and scintillator tiles read out with scintillating fibers radially along outside faces into PMTs

ATLAS hadronic calorimeters

$$\frac{\sigma_E}{E} = \frac{A}{\sqrt{E}} \oplus B \oplus \frac{C}{E}$$

ATLAS hadronic calorimeter $A \simeq 0.50,\ B \simeq 0.033,\ C = 0.018$

$$E = 1000\ \text{GeV} \quad \rightarrow \quad \frac{\sigma_E}{E} = 0.04$$

$$\frac{\sigma_p}{p} = 1.00$$

hadronic shower in ATLAS

- visible EM $\sim$ (50%)
  - $e,\ \gamma,\ \pi^0$
- visible non-EM $\sim$ (25%)
  - ionization of $\pi,\ p,\ \mu$
- invisible $\sim$ (25%)
  - nuclear break-up
  - nuclear excitation
- escaped $\sim$ (2%)

ATLAS hadronic calo: pion energy resolution

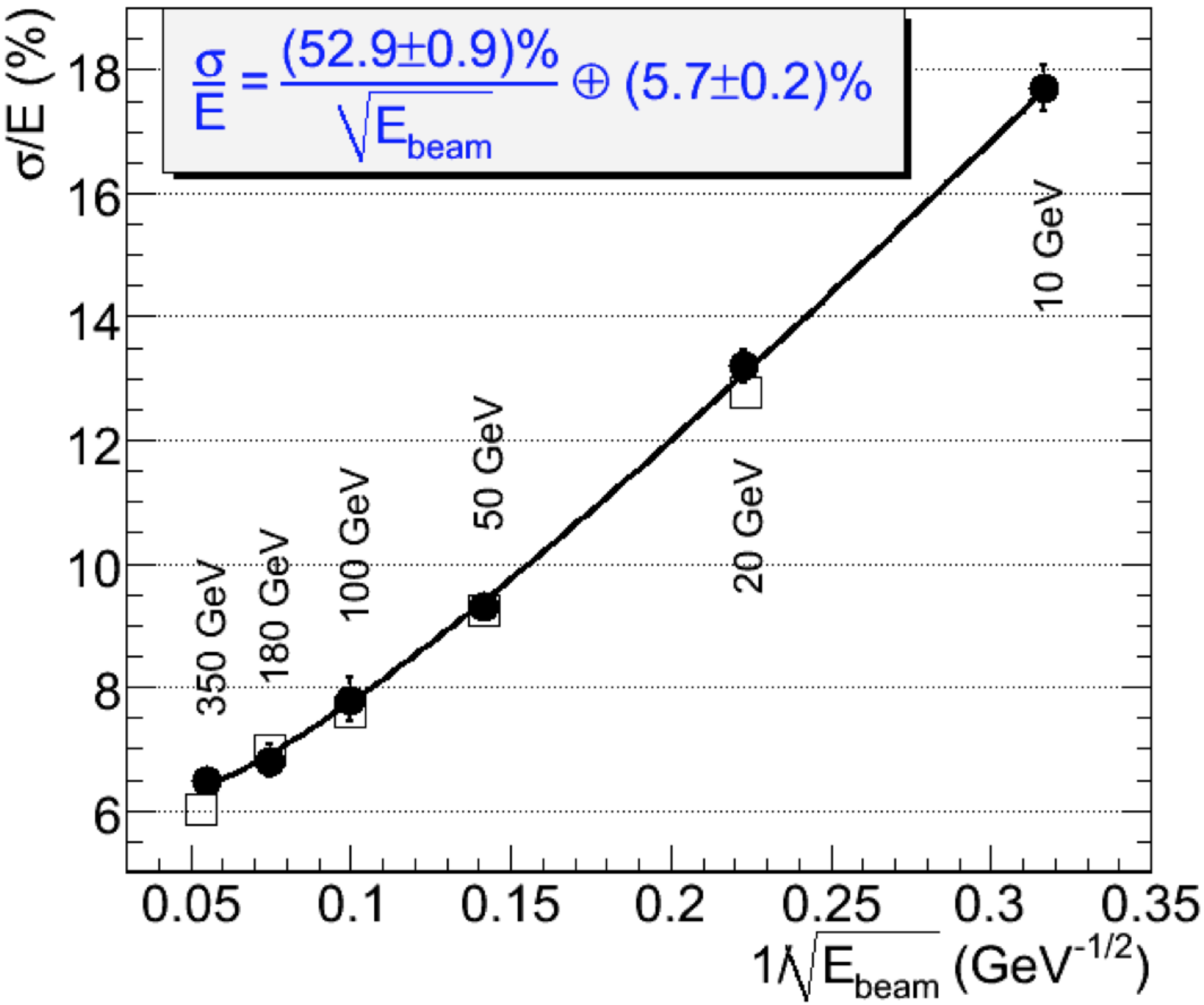

Calibration and monitoring of calorimeters

The pulse height A_i measured in an event from a certain (ith) element of the calorimeter is related to the energy E_i deposited in that element by

$$E_i = \alpha_i (A_i - P_i)$$

where P_i is the pedestal (i.e. the origin of the scale) and α_i is the calibration coefficient.

To keep good performance of the calorimeter, the following procedures are usually carried out:

- Pedestal determination by providing a trigger from a pulser without any signal at the input of the ADC ("random trigger events")
- Electronics channel control by test pulses applied to the input of the electronics chain
- Monitoring of the stability of the calibration coefficients α_i
- Absolute energy calibration, i.e. determination of the α_i values

Calibration and monitoring of calorimeters

Calibration by:

- Measure of a few modules of the final calorimeter in test beams of known particles (e, π, etc.) of known energy
  $\rightarrow$ intercalibration of all modules in the final calorimeter
- Use of very high energy muons from cosmic rays (might not manage to cover ALL modules, at all angles)
- Use of physical signals (e.g. decays, etc.)

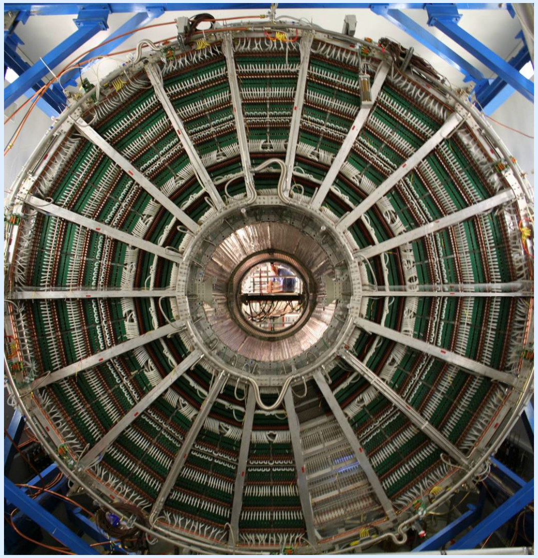

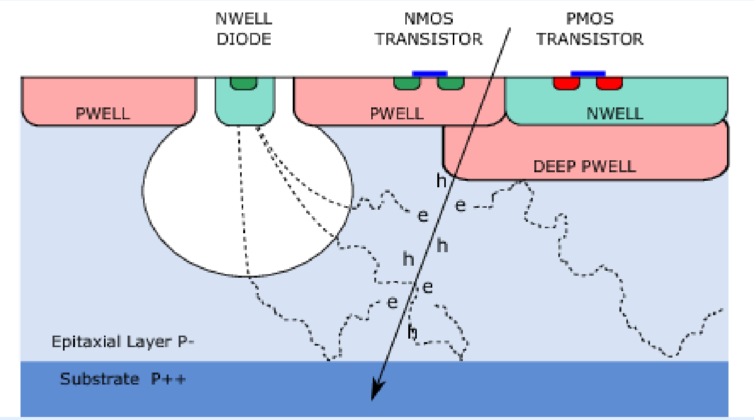
NWELL
DIODE
NMOS
TRANSISTOR
PMOS
TRANSISTOR
PWELL
PWELL
NWELL
DEEP PWELL
h
e
e
h
h
e
e
h
Epitaxial Layer P-
Substrate P++